AD693090

ARPA ORDER NO. 189-1

MEMORANDUM
RM-5830-ARPA
JULY 1969

PROPAGATION OF SOUND AS AFFECTED BY WIND AND TEMPERATURE GRADIENTS

R. H. Frick

PREPARED FOR:
ADVANCED RESEARCH PROJECTS AGENCY

DDC
RECEIVED
SEP 12 1969
C

The RAND Corporation
SANTA MONICA • CALIFORNIA

Reproduced by the
CLEARINGHOUSE
for Federal Scientific & Technical
Information Springfield Va. 22151

THIS DOCUMENT HAS BEEN APPROVED FOR PUBLIC RELEASE AND SALE; ITS DISTRIBUTION IS UNLIMITED.

94

ARPA ORDER NO. 189-1

MEMORANDUM
RM-5830-ARPA
JULY 1969

PROPAGATION OF SOUND AS AFFECTED BY WIND AND TEMPERATURE GRADIENTS

R. H. Frick

This research is supported by the Advanced Research Projects Agency under Contract No. DAHC15 67 C 0141. Views or conclusions contained in this study should not be interpreted as representing the official opinion or policy of ARPA.

DISTRIBUTION STATEMENT
This document has been approved for public release and sale; its distribution is unlimited.

The RAND Corporation
1700 MAIN ST • SANTA MONICA • CALIFORNIA • 90406

PREFACE

This Memorandum is part of a study requested by the Advanced Research Projects Agency of the utilization, cost and effectiveness of employing acoustic sensors as part of a U.S., Soviet, or Mainland China defense against a low-flying aircraft attack. The summary report of the study is given by the classified RAND Memorandum, RM-5713-ARPA, Acoustic Surveillance for Defense Against Low-Flying Aircraft (U), by R. M. Smith.

The results presented here on sound transmission through the atmosphere and the resulting sound intensity at ground level due to an elevated source should be of interest not only in the field of aircraft detection but also in the area of noise control.

SUMMARY

This Memorandum presents the results of a study of the propagation of sound in the atmosphere with particular emphasis on the determination of the sound intensity produced at ground level by an elevated source such as a low-flying aircraft. For the purposes of this study, a stratified atmosphere is assumed in which the temperature, wind velocity, and humidity are dependent only on the altitude.

A three-dimensional ray-tracing program is developed which not only determines the ray geometry and propagation time but also the variation of intensity along the ray. This computation of intensity takes into account the focusing effects due to atmospheric refraction as well as the atmospheric attenuation along the path.

The program is used to determine the ground-level sound intensity due to a source at an altitude of 500 ft radiating 100 kW (134 HP) of acoustical power. The intensity is determined as a function of ground range and azimuth relative to the source for three representative arctic meteorological conditions. The results show that in the absence of atmospheric absorption the intensity in the immediate vicinity of the source varies inversely as the square of the range from the source. However, as the range increases, atmospheric refraction can result in shadow zones of abnormally low intensity as well as regions in which focusing occurs with a consequent enhancement of intensity.

As a result, it appears that the detection range of an elevated source is extremely sensitive to azimuth of propagation as well as source altitude, power, and frequency. Thus even for the high intensity source assumed the detection range might be as short as 6000 ft.

CONTENTS

LIST OF FIGURES

LIST OF TABLES

BLANK PAGE

SYMBOLS

a = sound absorption coefficient (ft^{-1})

a_c = classical sound absorption coefficient

a_m = molecular sound absorption coefficient

a_r = average sound absorption coefficient in the r^{th} layer

C = refraction constant

C_V = specific heat of air at constant volume

C_i = vibrational specific heat of oxygen

D = distance measured along a ray from the source

ΔD_r = path length in traversing the r^{th} layer

f = acoustical frequency

H = ratio of water molecules to air molecules

h = Planck's constant

h_r = altitude of the top of the r^{th} layer

I = sound intensity with atmospheric attenuation

I_o = sound intensity with no atmospheric attenuation

K = reciprocal of the relaxation time of the first vibrational state of oxygen

k = Boltzmann's constant

M = number of the layer containing z_M

M_a = molecular weight of air

M_w = molecular weight of water

m = number of the layer containing z_m

n = number of the layer containing z

$\bar{n}_l$ = unit vector along the wave normal

P_o = acoustical power of the source

dP = differential power radiated into a solid angle $d\Omega$

$p(T)$ = vapor pressure of water as a function of temperature

R = radial distance from the source

R_o = universal gas constant

r_h = relative humidity

dr = differential displacement in the direction of $\nabla\Theta_o$

dS = cross section of a differential flow tube

ds = differential displacement in the direction of $\nabla\Phi_o$

T = absolute temperature

t = propagation time from source

$t(z)$ = propagation time from z_m to z

Δt_r = increment of $t(z)$ in the r^{th} layer

U_r = the smaller of z and h_r

u_r = the larger of z_m and h_{r-1}

V_r = still air sound velocity at altitude h_r

v = still air sound velocity

v_R = component of ray velocity in the xz plane

v_n = component of ray velocity along the wave normal

v_o = value of v at source

v_r = expression for v in the r^{th} layer

W_E = easterly component of wind velocity

W_N = northerly component of wind velocity

$W_{x,r}$ = x component of wind velocity at altitude h_r

$W_{y,r}$ = y component of wind velocity at altitude h_r

$\bar{w}$ = wind velocity vector

w_x = x component of $\bar{w}$

w_y = y component of $\bar{w}$

w_{xo} = value of w_x at source altitude

w_{yo} = value of w_y at source altitude

w_{xr} = expression for w_x in the r^{th} layer

w_{yr} = expression for w_y in the r^{th} layer

x = horizontal coordinate of the ray measured from the source in the direction of the initial wave normal azimuth

x_A = mol fraction of oxygen in air

$x(z)$ = x displacement of the ray from z_m to z

Δx_r = increment in $x(z)$ in the r^{th} layer

y = horizontal coordinate of the ray measured from the source normal to the initial wave normal azimuth

$y(z)$ = y displacement of the ray from z_m to z

Δy_r = increment in $y(z)$ in the r^{th} layer

z = altitude coordinate of the ray measured from ground level

z_M = maximum altitude along a ray

z_m = minimum altitude along a ray

z_o = source altitude

α_r = still air sound velocity gradient in the r^{th} layer

β_{xr} = gradient of w_x in the r^{th} layer

β_{yr} = gradient of w_y in the r^{th} layer

η = coefficient of viscosity of air

Θ_o = wave normal elevation angle at source

θ = wave normal elevation angle at an altitude z

θ_R = elevation angle of the ray at an altitude z

θ_r = elevation angle of the wave normal at an altitude h_r

μ = coefficient of heat conductivity of air

ρ = density of air

ρ_w = density of water vapor

ϕ_o = wave normal azimuth angle at source

ϕ_R = azimuth angle of the ray at an altitude z

$d\Omega$ = differential solid angle at source

$\bar{\omega}$ = angular velocity of the wave normal

I. INTRODUCTION

The purpose of this Memorandum is to determine the effect of atmospheric conditions on the acoustic detection of low-flying aircraft. There is no question that low-flying aircraft can produce high sound intensities at locations on the ground in the vicinity of the flight path. However, effective acoustic detection of such aircraft depends on how this ground-level sound intensity drops off with distance from the source. This Memorandum is primarily concerned with the effect of atmospheric conditions on the intensity of the sound reaching the ground at a given position relative to an elevated source of known acoustic power.

If the atmosphere through which the sound is propagated has a uniform temperature, no wind, and no dissipation, the acoustic rays emanating from the source are straight lines, and the resulting intensity at ground level is directly proportional to the acoustic power of the source and inversely proportional to the square of the slant range measured from the source. The existence of a uniform atmosphere of the type postulated above is highly unlikely and it seems more probable that the temperature would decrease with altitude while wind velocity would increase. In Ref. 1, Rayleigh shows that in the presence of a linear gradient of temperature or wind velocity with altitude, the acoustic rays emanating from a source approximate catenaries. Other investigators have refined these results by assuming an adiabatic lapse rate of temperature and a logarithmic increase of wind velocity with altitude. However, in spite of the curvature of the rays introduced by these gradients of temperature and wind velocity, the intensity at ground level differs very little from that obtained for a uniform atmosphere.

While such assumptions regarding the structure of the atmosphere have the advantage of providing closed-form solutions for the ray equations, it must be recognized that the real atmosphere is subject to large deviations from its average wind and temperature structure, particularly in the first few thousand feet of altitude where terrain conditions are a factor.

Since the present study is concerned with sound propagation in this lower altitude range, it is apparent that the use of an average atmosphere is unsatisfactory. Instead it is assumed that the atmosphere is horizontally stratified and that within any given stratum the temperature, humidity, and both horizontal components of wind velocity have linear gradients with altitude. In this way, the best available representation of the actual atmosphere based on the most current meteorological sounding can be incorporated into the computations rather than an idealized average condition.

In Section II the refraction law applying to this type of stratified atmosphere is developed and the differential equations for the determination of the ray paths are formulated in three dimensions. Given the initial ray direction at the source, these equations are solved for the x, y, and z coordinates of the ray paths as a function of the propagation time. In addition, a determination of the ray density and the atmospheric absorption makes it possible to determine the intensity at any point along the ray.

In Section III the method is used to determine the ray patterns and the ground intensity variations for several simple temperature and wind gradient conditions. Finally, three representative arctic weather profiles are selected and the ground intensity variations with range and azimuth are determined.

II. ANALYSIS

STATEMENT OF THE PROBLEM

At a given observer's position at ground level it is desired to determine the sound intensity resulting from a sound source of known acoustical power located at a specified altitude, range, and direction relative to the observer. It is assumed that the atmosphere through which the sound is propagated is horizontally stratified such that at any point the temperature, wind velocity, and humidity are functions only of the altitude. In addition it is assumed that there are no vertical wind components.

REFRACTION LAW

In order to describe the nature of sound propagation in a medium of the sort specified above, it is first necessary to determine the refraction law which applies.

In Fig. 1, the unit vector $\bar{n}_1$ represents the instantaneous direction of the wave normal at a given point of the sound wave front. The vector $\bar{v}$ is the still air sound velocity at the above location having a direction along $\bar{n}_1$ and a magnitude which depends on the local temperature. The resultant velocity of the specified point of the wave front is then given as $\bar{v}_R$, which is the vector sum of $\bar{v}$ and the local wind velocity, $\bar{w}$. Thus the propagation velocity normal to the wave front is given by

$$v_n = v + (\bar{w}_1 \cdot \bar{n}_1) \tag{1}$$

Since the velocity v_n varies over the wave front, it can be shown that the wave normal has an angular velocity, $\bar{\omega}$, given by

$$\bar{\omega} = \frac{d\bar{n}_1}{dt} = [\nabla v_n \times \bar{n}_1] \tag{2}$$

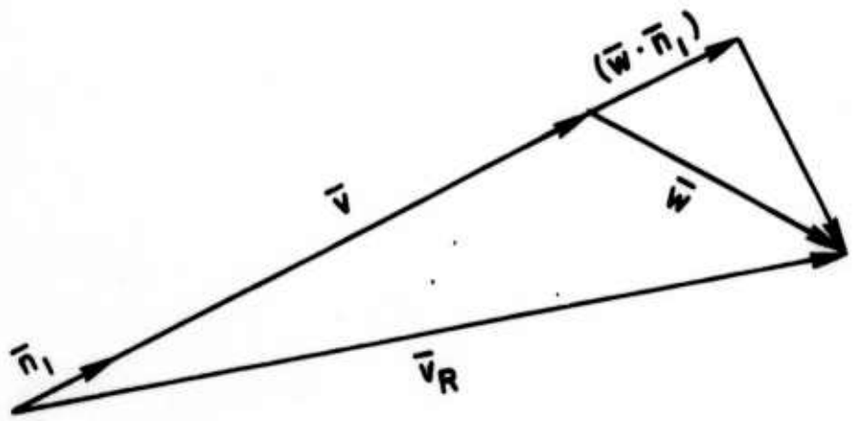

Fig. 1—Propagation geometry

If a coordinate system is selected with the z axis vertical and the unit vector $\bar{n}_1$ in the xz plane then

$$\bar{v} = v\bar{n}_1 \tag{3}$$

$$\bar{w} = w_x\bar{i} + w_y\bar{j} \tag{4}$$

$$\bar{n}_1 = \bar{i}\cos\theta + \bar{k}\sin\theta \tag{5}$$

where θ is the inclination of the wave normal to the horizontal.

On the assumption of a stratified atmosphere, the quantities v, w_x, and w_y are functions of z only. Equation (2) becomes

$$\bar{\omega} = \bar{j}\left(\frac{\partial v}{\partial z} + \frac{\partial w_x}{\partial z}\cos\theta\right)\cos\theta \tag{6}$$

Thus $\bar{n}_1$ rotates about the y axis and always remains parallel to the xz plane. Therefore Eq. (6) can be replaced by the scalar relation

$$\frac{d\theta}{dt} = -\left(\frac{\partial v}{\partial z} + \frac{\partial w_x}{\partial z}\cos\theta\right)\cos\theta \tag{7}$$

However, the angular rate $\frac{d\theta}{dt}$ can also be expressed as

$$\frac{d\theta}{dt} = \frac{\partial\theta}{\partial z}\frac{dz}{dt} = \frac{\partial\theta}{\partial z}v\sin\theta \tag{8}$$

Combination of Eqs. (7) and (8) gives

$$\frac{\frac{\partial\theta}{\partial z}v\sin\theta + \frac{\partial v}{\partial z}\cos\theta}{\cos^2\theta} + \frac{\partial w_x}{\partial z} = 0 \tag{9}$$

which can be integrated to give

$$\frac{v}{\cos \theta} + w_x = C \tag{10}$$

Equation (10) is the desired refraction law which specifies the variation of θ along a given ray as a function of altitude. The value of C which specifies the ray is determined from the initial conditions as

$$C = \frac{v_o}{\cos \Theta_o} + w_{xo} \tag{11}$$

where v_o, w_{xo}, and Θ_o are the values of v, w_x, and θ respectively at the source. For a fixed source altitude, the dependence of C on the initial wave normal elevation angle, Θ_o, is shown in Fig. 2.

The vertical component of the ray velocity $\bar{v}_R$ is given by

$$\frac{dz}{dt} = v \sin \theta \tag{12}$$

Thus if Θ_o is positive the ray rises initially and continues to rise until the angle θ reduces to zero. From Eq. (10) it is seen that this occurs at an altitude for which $v + w_x$ is equal to C. At this altitude it is found from Eq. (7) that

$$\frac{d\theta}{dt} = - \frac{\partial}{\partial z} (v + w_x) < 0 \tag{13}$$

so that θ becomes negative and from Eq. (12) the ray moves downward until it either reaches the ground or reaches an altitude below the source level at which $v + w_x$ is again equal to C. In this latter case it can be shown that θ becomes positive and the ray begins to rise again.

This behavior can be determined by plotting $v + w_x$ as a function of altitude as in Fig. 3, for example, where z_o is the source altitude. In this case, if Θ_o is zero the value of C is equal to C_o. It is seen that the resulting ray has a maximum altitude of z_o and a minimum altitude of z_o' and can never reach ground level. As C increases the

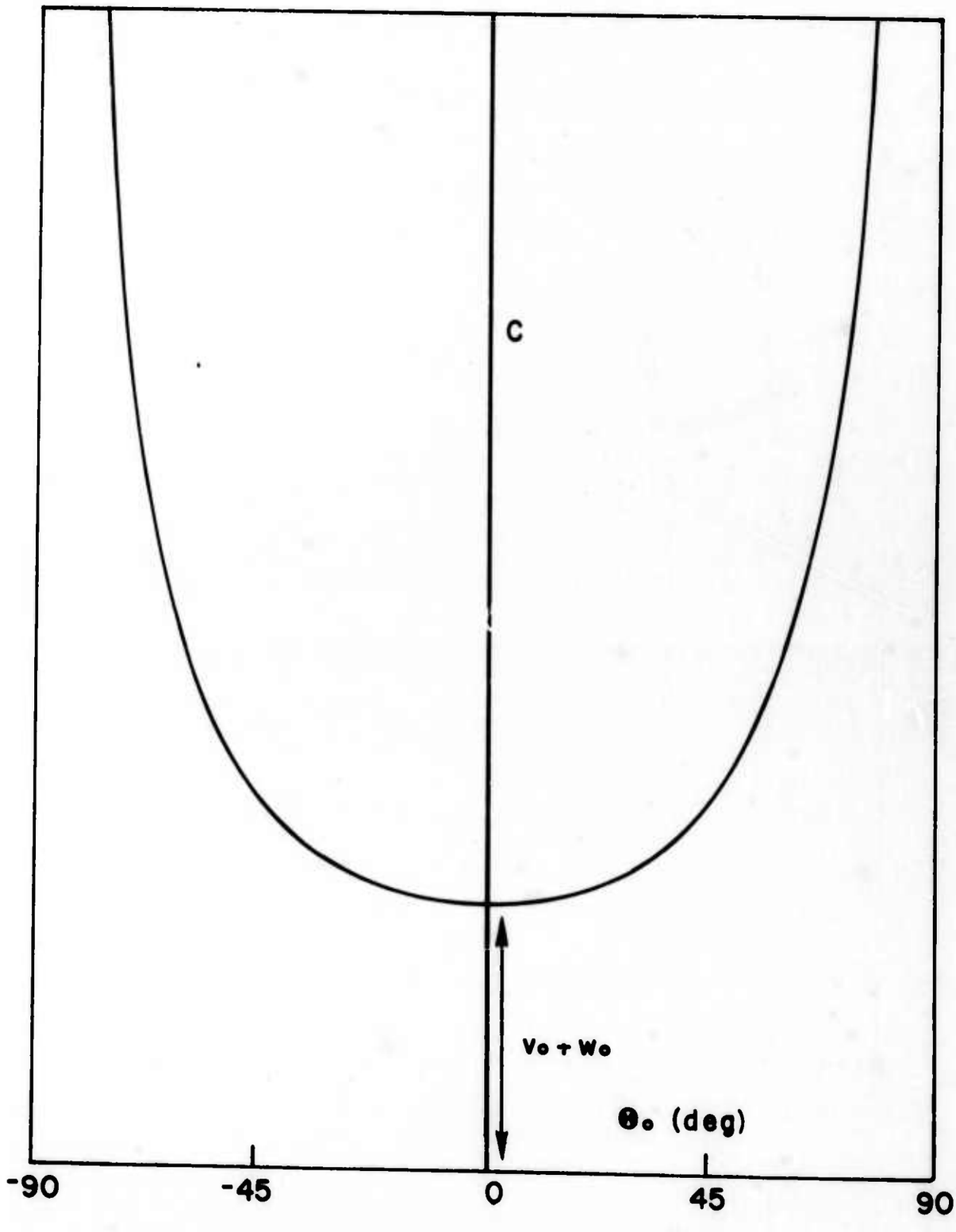

Fig. 2—Dependence of the refraction constant C on Θ_o

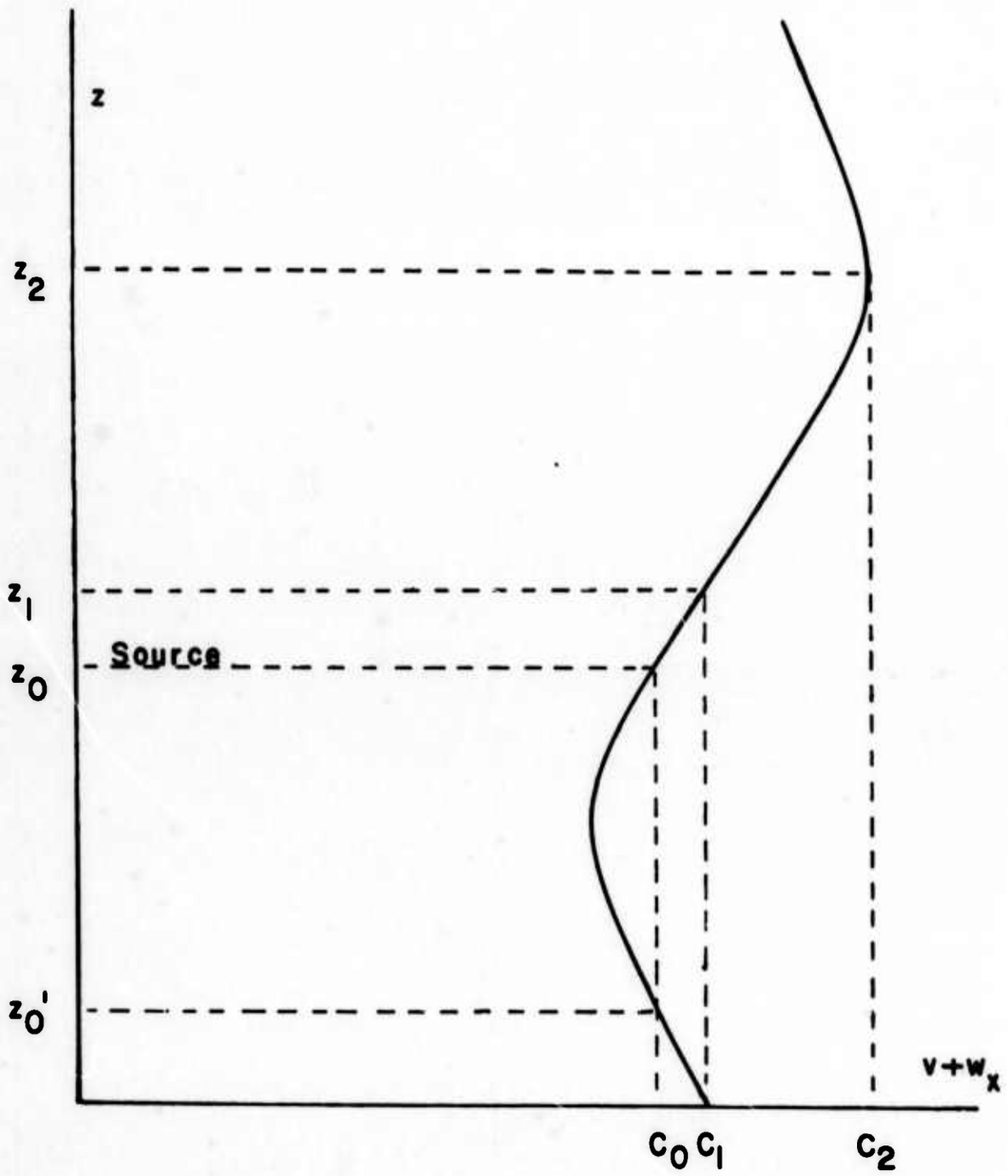

Fig. 3—Limitations on the altitude of a ray

maximum altitude increases and the minimum decreases until at a value of C_1 the ray reaches the ground at grazing incidence and reaches a maximum altitude of z_1. For values of C between C_1 and C_2, the maximum altitude lies between z_1 and z_2 while the minimum is at ground level. Finally, if C is greater than C_2, the maximum altitude is beyond the range of the indicated meteorological data while the minimum is still at ground level.

RAY DETERMINATION

The three component equations of the ray velocity can be expressed as

$$\frac{dx}{dt} = v \cos \theta + w_x \tag{14}$$

$$\frac{dy}{dt} = w_y \tag{15}$$

$$\frac{dz}{dt} = v \sin \theta \tag{16}$$

The determination of the ray involves the simultaneous solution of these equations, together with the refraction law, Eq. (10). It is convenient to select z as the independent variable so that the resulting solutions become

$$x(z) = \int_{z_m}^{z} \frac{v \cos \theta + w_x}{v \sin \theta} \, dz \tag{17}$$

$$y(z) = \int_{z_m}^{z} \frac{w_y}{v \sin \theta} \, dz \tag{18}$$

$$t(z) = \int_{z_m}^{z} \frac{dz}{v \sin \theta} \tag{19}$$

This form of the solution gives the variation of x, y, and t as the ray altitude, z, increases from its minimum value z_m to its maximum value z_M. While these expressions assume a rising ray, it will be shown that the x, y, and t values measured relative to the source can be expressed as a linear combination of x(z), y(z), and t(z) evaluated at z, z_o, and z_M even though the ray may pass through maxima and minima on the way.

In the previous section, it is assumed that v, w_x, and w_y are functions of z only. At this point it is further assumed that the atmosphere can be divided into horizontal layers such that in the r^{th} layer the quantities v, w_x, and w_y have linear gradients with altitude as follows:

$$v_r = V_{r-1} + \alpha_r \left(z - h_{r-1}\right) \tag{20}$$

$$w_{xr} = W_{x,r-1} + \beta_{xr} \left(z - h_{r-1}\right) \tag{21}$$

$$w_{yr} = W_{y,r-1} + \beta_{yr} \left(z - h_{r-1}\right) \tag{22}$$

if

$$h_{r-1} \leq z \leq h_r \tag{23}$$

In the above equations α_r, β_{xr}, and β_{yr} are gradients of v, w_x, and w_y respectively while V_{r-1}, $W_{x,r-1}$, and $W_{y,r-1}$ are the values of v, w_x, and w_y at h_{r-1}, the altitude of the bottom of the r^{th} layer.

With this specification of the meteorological conditions, Eqs. (17) through (19) can be integrated to give

$$x(z) = \sum_{r=m}^{n} \int_{u_r}^{U_r} \frac{v_r \cos\theta + w_{xr}}{v_r \sin\theta} \, dz = \sum_{r=m}^{n} \Delta x_r \tag{24}$$

$$y(z) = \sum_{r=m}^{n} \int_{u_r}^{U_r} \frac{w_{yr}}{v_r \sin\theta} \, dz = \sum_{r=m}^{n} \Delta y_r \tag{25}$$

$$t(z) = \sum_{r=m}^{n} \int_{u_r}^{U_r} \frac{dz}{v_r \sin\theta} = \sum_{r=m}^{n} \Delta t_r \tag{26}$$

where m and n are defined by the conditions that

$$h_{m-1} < z_m \leq h_m \tag{27}$$

and

$$h_{n-1} < z \leq h_n \tag{28}$$

Also, the limits of integration are defined as

$$U_r = \min (z, h_r)$$

$$u_r = \max (z_m, h_{r-1})$$

The evaluation of these integrals results in

$$\Delta x_r = x_r(U_r) - x_r(u_r) \tag{29}$$

$$\Delta y_r = y_r(U_r) - y_r(u_r) \tag{30}$$

$$\Delta t_r = t_r(U_r) - t_r(u_r) \tag{31}$$

where the functions $x_r(z)$, $y_r(z)$, and $t_r(z)$ are defined as follows:

$$x_r(z) = -\frac{1}{\alpha_r}\left[v_r \tan\theta - A_{xr} t_r(z)\right] \tag{32}$$

$$y_r(z) = -\frac{\beta_{yr} v_r}{\alpha_r\left(\beta_{xr}^2 - \alpha_r^2\right)\cos\theta}\left[\beta_{xr}\sin\theta + \alpha_r(\alpha_r + \beta_{xr}\cos\theta) I_r(z)\right]$$

$$+ \frac{1}{\alpha_r} A_{yr} t_r(z) \qquad \text{if } \beta_{xr}^2 \neq \alpha_r^2 \tag{33}$$

$$= -\frac{\beta_{yr} v_r}{3\alpha_r^2}\left[\frac{\cos\theta \pm 2}{\cos\theta}\right]\left(\tan\frac{\theta}{2}\right)^{\pm 1}$$

$$+ \frac{A_{yr}}{\alpha_r^2}\left[\log\left|\frac{\sin\frac{\theta}{2} - \cos\frac{\theta}{2}}{\sin\frac{\theta}{2} + \cos\frac{\theta}{2}}\right| \mp \alpha_r I_r(z)\right] \quad \text{if } \beta_{xr} = \pm\alpha_r \tag{34}$$

$$t_r(z) = \frac{1}{\alpha_r}\left[\log\left(\frac{1 - \sin\theta}{\cos\theta}\right) - \beta_{xr} I_r(z)\right] \tag{35}$$

where

$$I_r(z) = \frac{1}{\sqrt{\beta_{xr}^2 - \alpha_r^2}} \log\left|\frac{v_r\left(\sqrt{\beta_{xr}^2 - \alpha_r^2}\sin\theta - \alpha_r\cos\theta - \beta_{xr}\right)}{\cos\theta}\right|$$

$$\text{if } \beta_{xr}^2 > \alpha_r^2 \tag{36}$$

$$= \frac{1}{\sqrt{\alpha_r^2 - \beta_{xr}^2}} \sin^{-1}\left[\frac{\beta_{xr} + \alpha_r\cos\theta}{\beta_{xr}\cos\theta + \alpha_r}\right] \quad \text{if } \beta_{xr}^2 < \alpha_r^2 \tag{37}$$

$$= \mp \left(\tan \frac{\theta}{2}\right)^{\pm 1} \qquad \text{if } \beta_r = \pm \alpha_r \tag{38}$$

$$A_{xr} = \alpha_r W_{z,r-1} - \beta_{xr} V_{r-1} \tag{39}$$

$$A_{yr} = \alpha_r W_{y,r-1} - \beta_{yr} V_{r-1} \tag{40}$$

As indicated previously, the functions x(z), y(z), and t(z) are zero at z_m and assume that z is increasing. However, these functions can be used to determine the x, y, and t values measured from the source as follows:

If $\Theta_o > 0$ or $z_o = z_m$

$$x = x(z) - x(z_o) \quad \text{if} \quad z_o \le z \le z_M \quad \text{and} \quad \frac{dz}{dt} > 0 \tag{41}$$

$$= 2x(z_M) - x(z) - x(z_o) \quad \text{if} \quad \frac{dz}{dt} < 0 \tag{42}$$

$$= 2x(z_M) + x(z) - x(z_o) \quad \text{if} \quad z_m \le z < z_o \quad \text{and} \quad \frac{dz}{dt} > 0 \tag{43}$$

where z_M = maximum altitude of the ray.

Thus for these conditions, Eq. (41) determines the x displacement as z increases from z_o to z_M. If z_M is not infinite then Eq. (42) applies as z decreases from z_M to z_m. Finally, Eq. (43) is used as z increases from z_m to z_o, thus completing a full cycle of the altitude variation.

If $\Theta_o < 0$ or if $z_o = z_M$

$$x = x(z_o) - x(z) \quad \text{if} \quad z_o \ge z \ge z_m \quad \text{and} \quad \frac{dz}{dt} < 0 \tag{44}$$

$$= x(z_o) + x(z) \quad \text{if} \quad \frac{dz}{dt} > 0 \tag{45}$$

$$= 2x(z_M) + x(z_o) - x(z) \quad \text{if} \quad z_M \geq z \geq z_o \quad \text{and} \quad \frac{dz}{dt} < 0 \tag{46}$$

In this case Eq. (44) applies as z decreases from z_o to z_m, Eq. (45) determines the value of x as z increases from z_m to z_M and, finally, if z_M is not infinite, Eq. (46) is in effect as z decreases from z_M to z_o.

The corresponding expressions for y and t are obtained from Eqs. (41) through (46) by replacing x by y or t.

The foregoing analysis gives a complete solution for an acoustic ray traversing an atmosphere with a stratified wind and temperature structure in terms of the height of the source and the azimuth and elevation angles of the wave normal at the source.

INTENSITY DETERMINATION

Suppose that the wave normal corresponding to a particular ray has an elevation angle, Θ_o, and an azimuth angle, Φ_o (zero by definition), at the source. If this wave normal is perturbed by an amount $d\Theta_o$ in elevation and $d\Phi_o$ in azimuth, the resulting perturbations in in the elevation and azimuth angles, θ_R and ϕ_R, of the ray velocity are as shown in Figs. 4a and 4b. In these figures v_o, w_{xo}, and w_{yo} are the still air sound velocity and the two wind components at the source location. These perturbations, $d\theta_R$ and $d\phi_R$, can be used to define a differential solid angle $d\Omega$ at the source in the form

$$d\Omega = \cos \theta_R d\theta_R d\phi_R \tag{47}$$

or in the terms of Θ_o and Φ_o this becomes

$$d\Omega = \left(1 - \frac{w_{xo}}{v_o} \cos \Theta_o\right) \cos \Theta_o d\Theta_o d\Phi_o \tag{48}$$

Since $w_{xo} \ll v_o$, it is seen that the solid angle can be expressed to a good approximation as

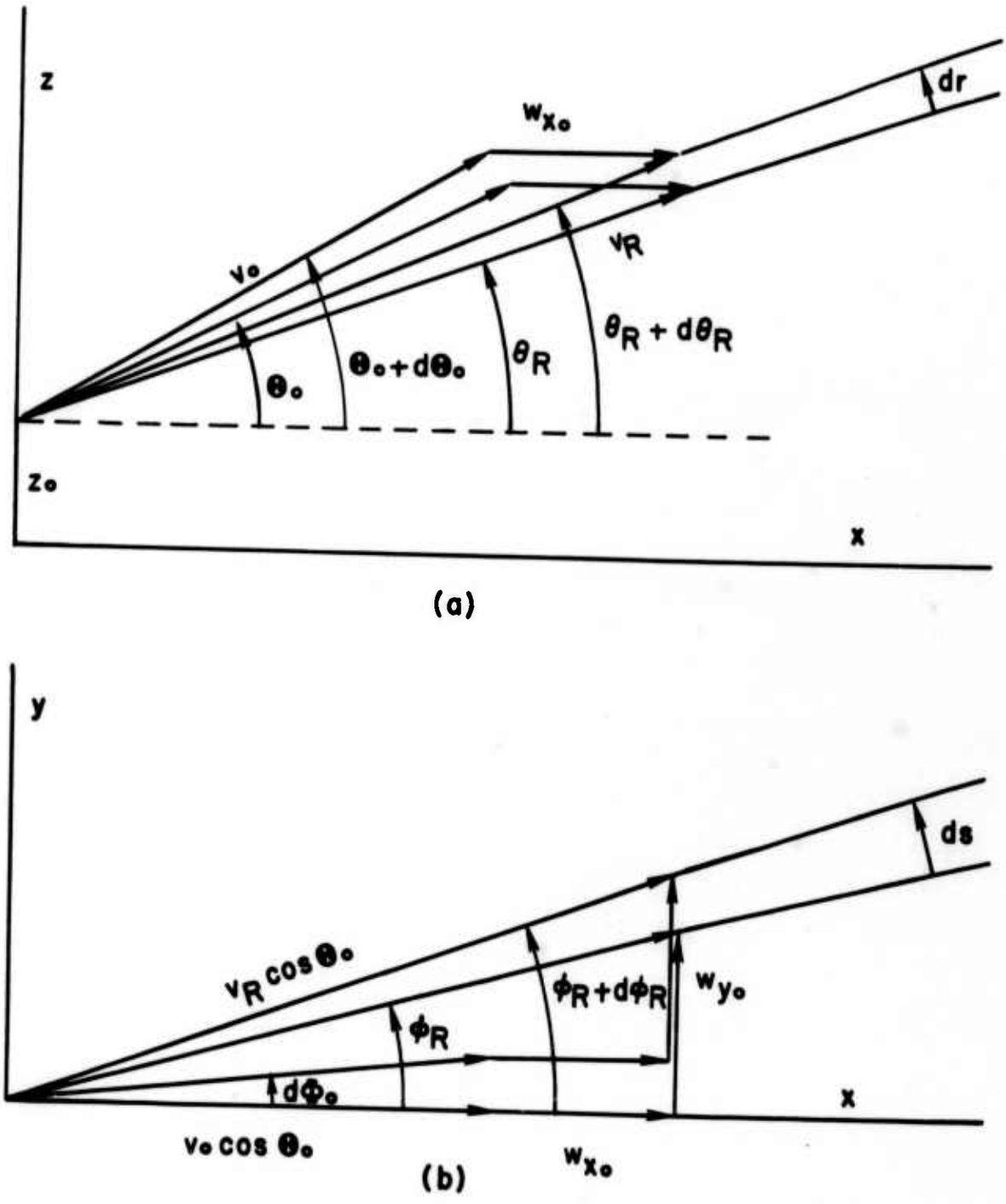

Fig. 4—Perturbations of a ray in elevation and azimuth

$$d\Omega = \cos \Theta_o d\Theta_o d\Phi_o \tag{49}$$

If the source is omnidirectional and has an acoustic power of P_o, then the energy flow rate from the solid angle $d\Omega$ is given by

$$dP = \frac{P_o}{4\pi} \cos \Theta_o d\Theta_o d\Phi_o \tag{50}$$

All of the energy flow from $d\Omega$ remains confined to a tube bounded by the family of acoustic rays which initially bounded the solid angle $d\Omega$. Figures 4a and 4b show the vertical and horizontal projections of this tube. Since no energy passes through the sides of the tube and it is assumed that there is no attenuation, the energy flow rate through any cross section must be equal to dP. Sound intensity is defined as the energy flow per second per unit of area normal to the direction of propagation, thus

$$dP = I_o dS \tag{51}$$

where I_o is the sound intensity and dS is the cross-sectional area of the flow tube. Combination of Eqs. (50) and (51) gives

$$I_o = \frac{P_o \cos \Theta_o d\Theta_o d\Phi_o}{4\pi\, dS} \tag{52}$$

The cross section dS is the product of dr, the width of the tube in the vertical plane, and ds, the width in the horizontal plane. Since dr depends only on $d\Theta_o$ and ds on $d\Phi_o$, Eq. (52) can be rewritten as

$$I_o = \frac{P_o \cos \Theta_o}{4\pi \left(\frac{dr}{d\Theta_o}\right)\left(\frac{ds}{d\Phi_o}\right)} \tag{53}$$

Thus it is seen that the sound intensity varies inversely as the area of the flow tube. For a constant temperature atmosphere with no wind the acoustic rays are straight lines radiating from the source and

$$\frac{dr}{d\Theta_o} = R \tag{54}$$

$$\frac{ds}{d\Phi_o} = R \cos \Theta_o \tag{55}$$

where R is the radial distance from the source. Equation (53) reduces to

$$I_o = \frac{P_o}{4\pi R^2} \tag{56}$$

the familiar inverse square variation of intensity with distance.

The equivalents to Eqs. (54) and (55) when wind and temperature gradients are present can be obtained as follows. Equations (41) through (46) define a family of acoustic rays in the xz plane with Θ_o constant for a given ray. Thus

$$\frac{dr}{d\Theta_o} = \frac{1}{|\nabla\Theta_o|} \tag{57}$$

where

$$\nabla\Theta_o = \frac{\sqrt{1 + \left(\frac{\partial x}{\partial z}\right)^2}}{\left(\frac{\partial x}{\partial \Theta_o}\right)} \tag{58}$$

An examination of Eqs. (41) through (46) shows that the general form of the ray equations is

$$x = \pm\, x(z) + F(z_o, z_m, z_M) \tag{59}$$

where the function F is a linear combination of $x(z_o)$, $x(z_m)$, and $x(z_M)$. From Eqs. (17) and (59) it is seen that

$$\frac{\partial x}{\partial z} = \pm \frac{\partial x(z)}{\partial z} = \pm \frac{v \cos \theta + w_x}{v \sin \theta} \tag{60}$$

and

$$\frac{\partial x}{\partial \Theta_o} = \pm \frac{\partial x(z)}{\partial \Theta_o} + \frac{\partial F(z_o, z_m, z_M)}{\partial \Theta_o} \tag{61}$$

Thus Eq. (57) can be written as

$$\frac{dr}{d\Theta_o} = \frac{v \sin \theta}{v_R} \left| \pm \frac{\partial x(z)}{\partial \Theta_o} + \frac{\partial F}{\partial \Theta_o} \right| \tag{62}$$

where v_R is the component of the ray velocity in the xz plane and is given by

$$v_R = \sqrt{v^2 + w_x^2 + 2v\, w_x \cos \theta} \tag{63}$$

The derivative of x(z) with respect to Θ_o can be expressed by means of Eq. (11) in the form

$$\frac{\partial x(z)}{\partial \Theta_o} = \frac{v_o \sin \Theta_o}{\cos^2 \Theta_o} X(z) \tag{64}$$

where from Eq. (24)

$$X(z) = \sum_{r=m}^{n} \frac{\partial \Delta x_r}{\partial C} \tag{65}$$

and

$$\frac{\partial \Delta x_r}{\partial C} = \frac{C}{\left[(C - W_{xm})\ \alpha_m + V_m \beta_{xm}\right]} \left[- \frac{1}{\sin\ \theta(U_m)} \right] \quad \text{if } r = m \tag{66}$$

$$= \frac{C}{\left[(C - W_{xr})\ \alpha_r + V_r \beta_{xr}\right]} \left[\frac{1}{\sin\ \theta(u_r)} - \frac{1}{\sin\ \theta(U_r)} \right]$$

$$\text{if} \quad r \neq m \quad \text{and} \quad \left[(C - W_{xr})\ \alpha_r + V_r \beta_{xr}\right] \neq 0 \tag{67}$$

$$= \frac{C \gamma_r^2}{\left(\alpha_r^2 - \beta_{xr}^2\right)^{3/2}} \left[\frac{1}{v(U_r)} - \frac{1}{v(u_r)} \right]$$

$$\text{if} \quad \left[(C - W_{xr})\ \alpha_r + V_r \beta_{xr}\right] = 0 \tag{68}$$

$$= \frac{C}{\left[(C - W_{xM})\ \alpha_M + V_M \beta_{xM}\right]} \left[\frac{1}{\sin\ \theta(u_M)} \right]$$

$$\text{if} \quad r = M \quad \text{and} \quad z = z_M \tag{69}$$

Since the function F is a linear combination of $x(z_o)$, $x(z_m)$, and $x(z_M)$, its partial derivative in Eq. (62) is a similar linear combination of $X(z_o)$, $X(z_m)$, and $X(z_M)$. These three quantities can be determined from the definition of X(z) above. Thus Eq. (62) can be expressed as follows:

If $\Theta_o > 0$ or if $z_o = z_m$

$$\frac{dr}{d\Theta_o} = \left| \frac{vv_o \sin\theta \sin\Theta_o}{v_R \cos^2\Theta_o} \left[X(z) - X(z_o) \right] \right|$$

$$\text{if} \quad z_o \le z \le z_M \quad \text{and} \quad \frac{dz}{dt} > 0 \tag{70}$$

$$= \left| \frac{vv_o \sin\theta \sin\Theta_o}{v_R \cos^2\Theta_o} \left[2X(z_M) - X(z) - X(z_o) \right] \right| \quad \text{if} \ \frac{dz}{dt} < 0 \tag{71}$$

$$= \left| \frac{vv_o \sin\theta \sin\Theta_o}{v_R \cos^2\Theta_o} \left[2X(z_M) + X(z) - X(z_o) \right] \right|$$

$$\text{if} \quad z_m \le z < z_o \quad \text{and} \quad \frac{dz}{dt} > 0 \tag{72}$$

If $\Theta_o < 0$ or $z_o = z_M$

$$\frac{dr}{d\Theta_o} = \left| \frac{vv_o \sin\theta \sin\Theta_o}{v_R \cos^2\Theta_o} \left[X(z_o) - X(z) \right] \right|$$

$$\text{if} \quad z_o \ge z \ge z_m \quad \text{and} \quad \frac{dz}{dt} < 0 \tag{73}$$

$$= \left| \frac{vv_o \sin\theta \sin\Theta_o}{v_R \cos^2\Theta_o} \left[X(z_o) + X(z) \right] \right| \quad \text{if} \ \frac{dz}{dt} > 0 \tag{74}$$

$$= \left| \frac{vv_o \sin\theta \sin\Theta_o}{v_R \cos^2\Theta_o} \left[2X(z_M) + X(z_o) - X(z) \right] \right|$$

$$\text{if} \quad z_M \ge z \ge z_o \quad \text{and} \quad \frac{dz}{dt} < 0 \tag{75}$$

It should be noted that Eqs. (70) through (75) become indeterminate if either θ or Θ_o is zero. However, this can be resolved as follows. If z approaches z_M in either Eq. (70) or (71), the bracketed terms are dominated by the M^{th} term in X(z), which from Eq. (67) is

$$\frac{\partial \Delta x_M}{\partial C} = \frac{C}{(C - W_{xM})\,\alpha_M + V_M \beta_{xM}} \left[\frac{1}{\sin \theta_{M-1}} - \frac{1}{\sin \theta} \right] \tag{76}$$

and as θ becomes small

$$\frac{\partial \Delta x_M}{\partial C} = - \frac{C}{v(\alpha_M + \beta_{xM}) \sin \theta} \tag{77}$$

Thus either Eq. (70) or (71) approaches a limit of

$$\frac{dr}{d\Theta_o} = \left| \frac{v_o \sin \Theta_o}{(\alpha_M + \beta_{xM}) \cos^2 \Theta_o} \right| \tag{78}$$

as z approaches z_M. In a similar manner it can be shown that as z approaches z_m, Eqs. (71) and (72) approach a limit of

$$\frac{dr}{d\Theta_o} = \left| \frac{v_o \sin \Theta_o}{(\alpha_m + \beta_{xm}) \cos^2 \Theta_o} \right| \tag{79}$$

It can also be shown that Eqs. (73) and (74) approach the limit given by Eq. (70) as z approaches z_m, while Eqs. (74) and (75) approach the limit given in Eq. (78) as z approaches z_M.

If z_o approaches z_m and Θ_o approaches zero, Eq. (70) reduces to

$$\frac{dr}{d\Theta_o} = \left| \frac{Cv \sin \theta}{v_R (\alpha_m + \beta_{xm})} \right| \tag{80}$$

as does Eq. (71).

Similarly as z_o approaches z_M and Θ_o approaches zero, both Eqs. (73) and (74) reduce to

$$\frac{dr}{d\Theta_o} = \left| \frac{Cv \sin \theta}{v_R(\alpha_M + \beta_{xM})} \right| \tag{81}$$

The other derivative in the denominator of Eq. (53) can be expressed as

$$\frac{ds}{d\Phi_o} = \frac{1}{|\nabla \Phi_o|} \tag{82}$$

Since

$$\left(\frac{\partial \Phi_o}{\partial x}\right)_y = \frac{\left(\frac{\partial y}{\partial z}\right)_{\Phi_o}}{\left(\frac{\partial x}{\partial \Phi_o}\right)_z \left(\frac{\partial y}{\partial z}\right)_{\Phi_o} - \left(\frac{\partial x}{\partial z}\right)_{\Phi_o} \left(\frac{\partial y}{\partial \Phi_o}\right)_z} \tag{83}$$

and

$$\left(\frac{\partial \Phi_c}{\partial y}\right)_x = \frac{\left(\frac{\partial x}{\partial z}\right)_{\Phi_o}}{\left(\frac{\partial x}{\partial \Phi_o}\right)_z \left(\frac{\partial y}{\partial z}\right)_{\Phi_o} - \left(\frac{\partial x}{\partial z}\right)_{\Phi_o} \left(\frac{\partial y}{\partial \Phi_o}\right)_z} \tag{84}$$

then Eq. (82) can be written as

$$\left(\frac{ds}{d\Phi_o}\right) = \left| \left(\frac{\partial x}{\partial \Phi_o}\right)_z \sin \phi_R - \left(\frac{\partial y}{\partial \Phi_o}\right)_z \cos \phi_R \right| \tag{85}$$

where

$$\sin \phi_R = \frac{\left(\frac{\partial y}{\partial z}\right)_{\Phi_o}}{\sqrt{\left(\frac{\partial x}{\partial z}\right)^2_{\Phi_o} + \left(\frac{\partial y}{\partial z}\right)^2_{\Phi_o}}} \tag{86}$$

and

$$\cos \phi_R = \frac{\left(\frac{\partial x}{\partial z}\right)_{\Phi_o}}{\sqrt{\left(\frac{\partial x}{\partial z}\right)^2_{\Phi_o} + \left(\frac{\partial y}{\partial z}\right)^2_{\Phi_o}}} \tag{87}$$

Since x is a linear combination of $x(z)$, $x(z_o)$, and $x(z_M)$, and y is a linear combination of $y(z)$, $y(z_o)$, and $y(z_M)$, their partial derivatives in Eq. (85) are similar linear combinations of the partials of $x(z)$ and $y(z)$ evaluated at z, z_o, and z_M. If Eqs. (17) and (18) for $x(z)$ and $y(z)$ are generalized to include Φ_o as follows:

$$x(z) = \int_{z_m}^{z} \frac{v \cos \theta \cos \Phi_o + w_x}{v \sin \theta} dz \tag{88}$$

$$y(z) = \int_{z_m}^{z} \frac{v \cos \theta \sin \Phi_o + wy}{v \sin \theta} dz \tag{89}$$

then

$$\left(\frac{\partial x(z)}{\partial \Phi_o}\right)_z = - \int_{z_m}^{z} \frac{\cos \theta \sin \Phi_o}{\sin \theta} dz \tag{90}$$

and

$$\left(\frac{\partial y(z)}{\partial \Phi_o}\right)_z = \int_{z_m}^{z} \frac{\cos\theta \cos\Phi_o}{\sin\theta}\, dz \tag{91}$$

When Φ_o is set equal to zero, Eqs. (90) and (91) become

$$\left(\frac{\partial x(z)}{\partial \Phi_o}\right)_z = 0 \tag{92}$$

$$\left(\frac{\partial y(z)}{\partial \Phi_o}\right)_z = \int_{z_m}^{z} \frac{\cos\theta\, dz}{\sin\theta} \tag{93}$$

Combination of Eqs. (88) and (93) gives

$$\left(\frac{\partial y(z)}{\partial \Phi_o}\right)_z = x(z) - \int_{z_m}^{z} \frac{w_x dz}{v \sin\theta} \tag{94}$$

Since $w_x \ll v$, the integral term can be neglected and if Eq. (91) is substituted into the expressions for y corresponding to Eqs. (41) through (46), it is found that

$$\frac{\partial y}{\partial \Phi_o} \doteq x \tag{95}$$

Thus Eq. (53) for the sound intensity becomes

$$I_o = \frac{P_o \cos\Theta_o}{4\pi x \left(\frac{dr}{d\Theta_o}\right)} \tag{96}$$

ATTENUATION

Dissipation of energy in the medium results in an exponential decrease of intensity with path length of the form

$$I = I_o e^{-aD} \tag{97}$$

where I_o is the intensity at a given location in the absence of any energy dissipation, D is the path length in the medium, and a is the sound absorption coefficient.

The principal causes of sound absorption in the atmosphere are viscosity, heat conductivity, and molecular absorption. Of these, the first two are ordinarily called classical absorption, for which the absorption coefficient, a_c, can be expressed as

$$a_c = \frac{4\pi^2 f^2}{\rho v^3}\left[\frac{4\eta}{3} + \frac{\mu M_w R_o}{C_V(C_V + R_o)}\right] \tag{98}$$

where

f = frequency of the sound wave (cycles/sec)

ρ = atmospheric density (gm/cm^3)

v = sound velocity (cm/sec)

η = coefficient of viscosity of air (poise)

μ = coefficient of heat conductivity of air ($cal/gm/^oC$)

M_w = molecular weight of air (gm/mol)

R_o = gas constant (cal/mol)

C_V = specific heat of air at constant volume ($cal/mol/^oC$)

a_c = absorption coefficient (1/cm)

Molecular absorption is due to the excitation by the sound wave of the vibrational states of the oxygen molecules in the atmosphere. The absorption coefficient in this case is given by

$$a_m = \frac{2\pi R_o x_A C_i}{C_o C_V (C_V + R_o)} \times \frac{Kf^2}{(f^2 + K^2)} \tag{99}$$

where

x_A = mol fraction of oxygen in air

C_i = vibrational specific heat of oxygen (cal/mol/^oC)

K = reciprocal of the relaxation time of the first vibrational state of oxygen (1/sec)

a_m = molecular absorption coefficient (1/cm)

The vibrational specific heat can be determined as a function of temperature from the expression (Eq. (263) of Ref. 2).

$$C_i = R_o \left(\frac{h\nu}{kT}\right)^2 \frac{e^{\frac{h\nu}{kT}}}{\left(e^{\frac{h\nu}{kT}} - 1\right)^2} \tag{100}$$

where T is the absolute temperature and from spectroscopic data $h\nu/k$ is equal to 2228 (Table 2 of Ref. 2).

In Refs. 3 and 4, it is shown that the value of the relaxation time of the first vibrational mode of oxygen depends on the amount of water vapor present. As a result the parameter K is given by the relation

$$K = 5.758 \times 10^8 H^2 \tag{101}$$

where H is the ratio of the number of water molecules to the number of air molecules and is given by

$$H = \frac{M_a \rho_w T}{M_w \rho_o T_o} \tag{102}$$

where

M_a = molecular weight of air

M_w = molecular weight of water

ρ_w = density of water vapor

ρ_o = air density at 0^oC

T_o = 273^oK

T = absolute temperature

Finally, ρ_w can be expressed as

$$\rho_w = \frac{M_w r_h p(T)}{R_o T} \tag{103}$$

where

r_h = relative humidity

$p(T)$ = water vapor pressure as a function of temperature

Thus the absorption coefficient α in Eq. (97) is the sum of α_c and α_m. However, for the stratified atmosphere assumed previously, α varies with altitude because of its dependence on both temperature and humidity; thus a more accurate representation of Eq. (97) is

$$I = I_o e^{-\int_o^D \alpha dD} = I_o e^{-A} \tag{104}$$

The integral in the exponent can be approximated if it is assumed that in the r^{th} layer of the atmosphere the absorption coefficient has a constant value, a_r, which corresponds to the average temperature and humidity for that layer. In addition, it is assumed that the length of the ray path in the r^{th} layer can be approximated as

$$\Delta D_r = \sqrt{\Delta x_r^2 + (U_r - u_r)^2} \tag{105}$$

If a function A(z) is defined as

$$A(z) = \sum_{r=m}^{n} a_r \Delta D_r \tag{106}$$

Then the integral in Eq. (104) can be expressed as follows.

If $\Theta_o > 0$ or $z_o = z_m$

$$A = A(z) - A(z_o) \quad \text{if} \quad z_o \le z \le z_M \quad \text{and} \quad \frac{dz}{dt} > 0 \tag{107}$$

$$= 2A(z_M) - A(z) - A(z_o) \quad \text{if} \quad \frac{dz}{dt} < 0 \tag{108}$$

$$= 2A(z_M) + A(z) - A(z_o) \quad \text{if} \quad z_m \le z \le z_o \quad \text{and} \quad \frac{dz}{dt} > 0 \tag{109}$$

If $\Theta_o < 0$ or $z_o = z_M$

$$A = A(z_o) - A(z) \quad \text{if} \quad z_o \ge z \ge z_m \quad \text{and} \quad \frac{dz}{dt} < 0 \tag{110}$$

$$= A(z_o) + A(z) \quad \text{if} \quad \frac{dz}{dt} > 0 \tag{111}$$

$$= 2A(z_M) + A(z_o) - A(z) \quad \text{if} \quad z_M \ge z \ge z_o \quad \text{and} \quad \frac{dz}{dt} < 0 \tag{112}$$

If Eqs. (96) and (104) are combined, the resulting expression for the sound intensity becomes

$$I = \frac{P_o \cos \Theta_o}{4\pi x \left(\frac{dr}{d\Theta_o}\right)} e^{-A} \tag{113}$$

COMPUTER PROGRAM

The foregoing analysis has been programmed for the JOSS* computer, a remote console, time-sharing computing system developed at The RAND Corporation. In this program the stratified atmosphere is specified by inputting the altitudes of the boundaries of the strata and the values of the still air sound velocity, the north and east components of wind velocity, and the relative humidity at each of these altitudes. The initial conditions for a given ray include the specification of the source altitude, the initial azimuth and elevation angles of the wave normal, and the acoustic power of the source.

Given the above inputs, the computer determines the x and y coordinates of the ray and the propagation time, t, for specified equal increments in ray altitude. In addition, at each point the sound intensity in dB relative to 10^{-16} watts/cm^2 is computed for frequencies of 125, 250, 500, and 1000 cps. This procedure continues until the ray either reaches the ground or the maximum altitude for which meteorological data are supplied.

While the program in its general form provides a complete three-dimensional solution for the geometry of the ray field as well as the intensity variations, it was soon found that for the purposes of this Memorandum the program could be simplified by neglecting the lateral or y displacement of the ray since it has very little effect on the variation of intensity with distance at ground level. Thus the program was split into two parts, one of which determines the x coordinates of the ray as well as the propagation time as a function of the ray altitude, z, while the second part computes the sound intensity at ground level as a function of horizontal distance from the source. This simplification shortens the solution time considerably with a negligible effect on the accuracy of the results.

---

*JOSS is the trademark and service mark of The RAND Corporation for its computer program and services using that program.

III. RESULTS

It is now of interest to apply the foregoing analysis under various meteorological conditions. For all of the cases considered in this section a source with an acoustical power of 100 kW (134 HP)* at an altitude of 500 ft is assumed.

BASIC EXAMPLES

Before considering any actual meteorological profiles, it is useful to examine a few simple cases.

Case 1

In this case the meteorological conditions assumed are shown below.

Altitude (ft)	Sound Velocity (ft/sec)	W_N (ft/sec)	W_E (ft/sec)
0	1100	0	0
2000	1085	0	0

W_N and W_E are the northerly and easterly wind components. Under this condition of a negative gradient of sound velocity and no wind, the rays emanating from the assumed source are as shown in Fig. 5, where it is seen that all of the rays are concave upward due to the negative gradient of sound velocity. In particular, for an initial wave normal elevation of -4.73 deg the corresponding sound ray is tangent to the ground at a range 12,100 ft and no rays reach the ground beyond this range, thus creating a shadow zone. In Fig. 6 the corresponding variation of sound intensity with range is shown. It is seen that the drop-off is still essentially an inverse-square-law variation with range out to 12,100 ft. Beyond this point, the ray theory indicates

*This acoustic power level is representative of a B-52 with a thrust level of 10,000 lb and a mass flow rate of 180 lb/sec for each of its 8 engines (see Fig. 33.42 of Ref. 5).

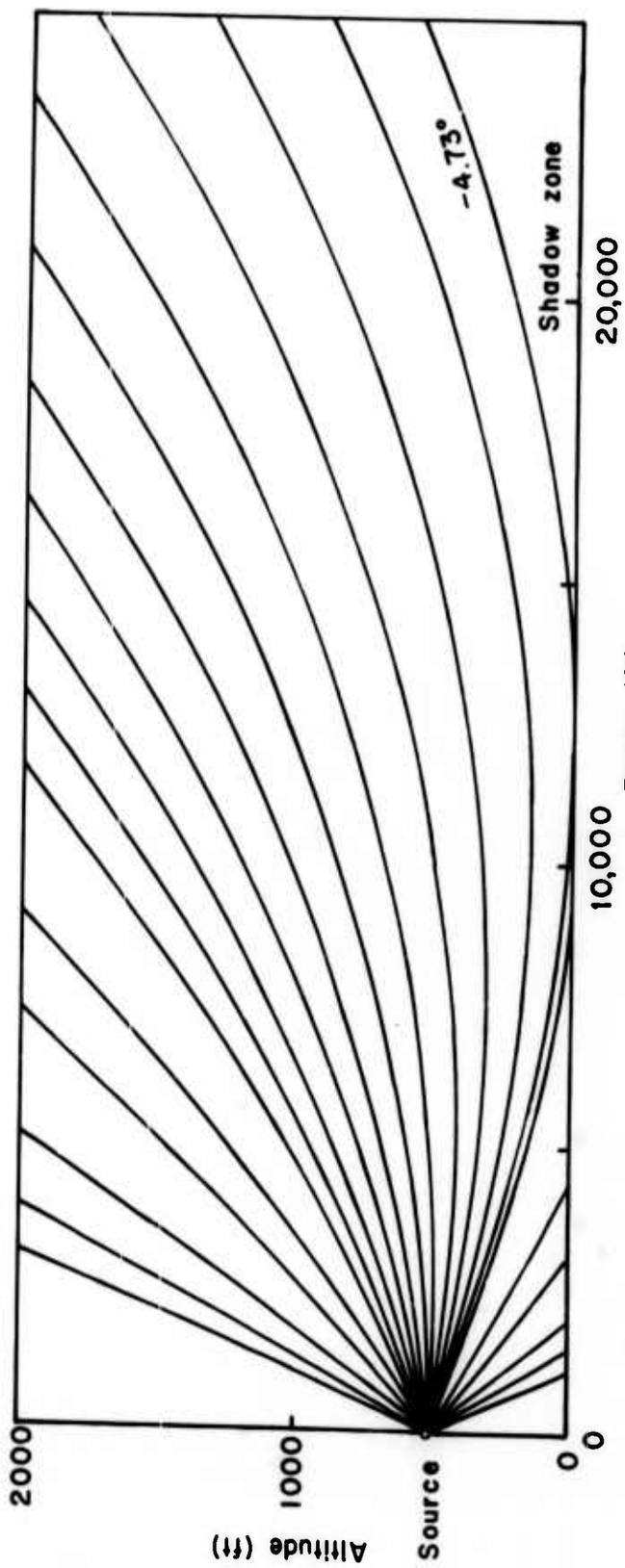

Fig. 5—Ray pattern (Case 1)

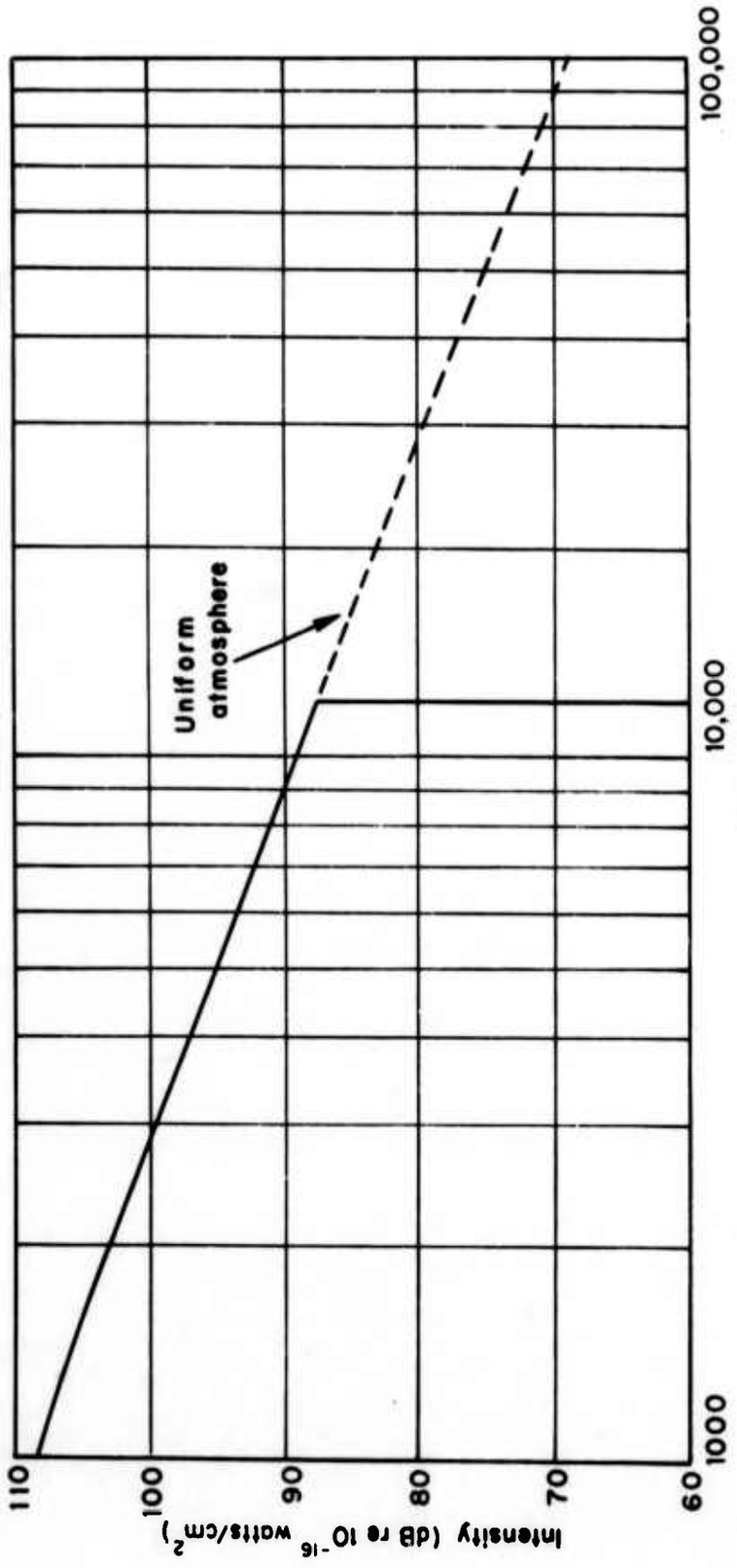

Fig. 6—Intensity variation with range (Case 1)

zero intensity; however, if the effects of diffraction and scattering are taken into account (see Refs. 6 and 7) the intensity in the shadow region, while no longer zero, still drops off much faster than an inverse-square-law variation.

It should be noted that the patterns shown in Figs. 5 and 6 are independent of the azimuth of propagation.

Case 2

In this case the meteorological conditions assumed are shown below.

Altitude (ft)	Sound Velocity (ft/sec)	W_N (ft/sec)	W_E (ft/sec)
0	1100	0	0
2000	1115	0	0

Under these conditions of a positive sound velocity gradient with altitude and again no wind, the resulting ray pattern is as shown in Fig. 7. Due to the positive gradient of sound velocity all of the rays are concave toward the earth. Thus no shadow zone is produced and long-range propagation should be expected. The variation of intensity with distance for this case is shown in Fig. 8 and again differs very little from the usual inverse-square-law decrease. As in the previous example, both Figs. 7 and 8 are independent of the azimuth of propagation.

In this case it is entirely possible that sound energy might reach a given observer along a number of different ray paths involving one or more reflections off the earth's surface. Under this condition of multipath transmission, known as surface ducting, it can be shown that at long ranges the intensity varies inversely as the first power of the range instead of the usual inverse-square law. However, for the elevated source specified, the first multiple arrival would be at a range of about 36,000 ft and it is probable that the inverse-first-power variation of intensity would not appear short of 100,000 ft range. Thus it appears that for the ranges considered here ducting has relatively little effect on the intensity, as shown in Fig. 8.

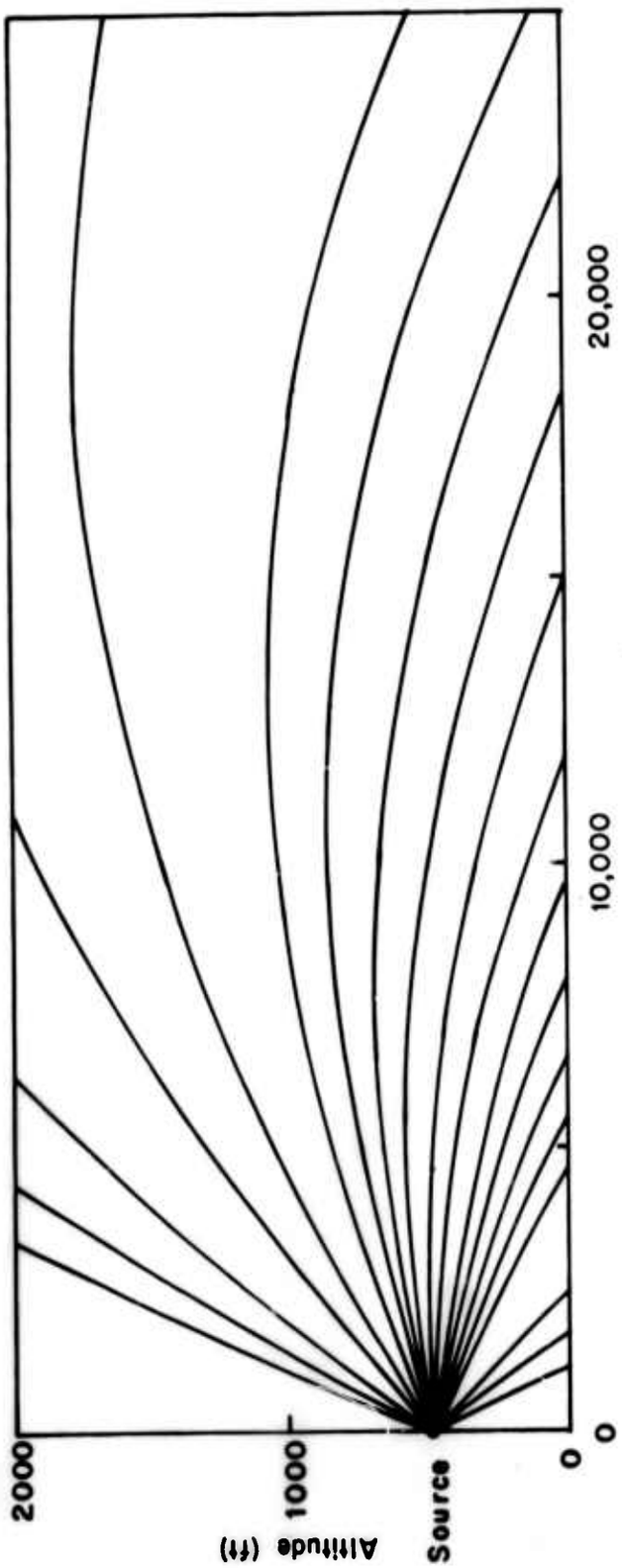

Fig. 7—Ray pattern (Case 2)

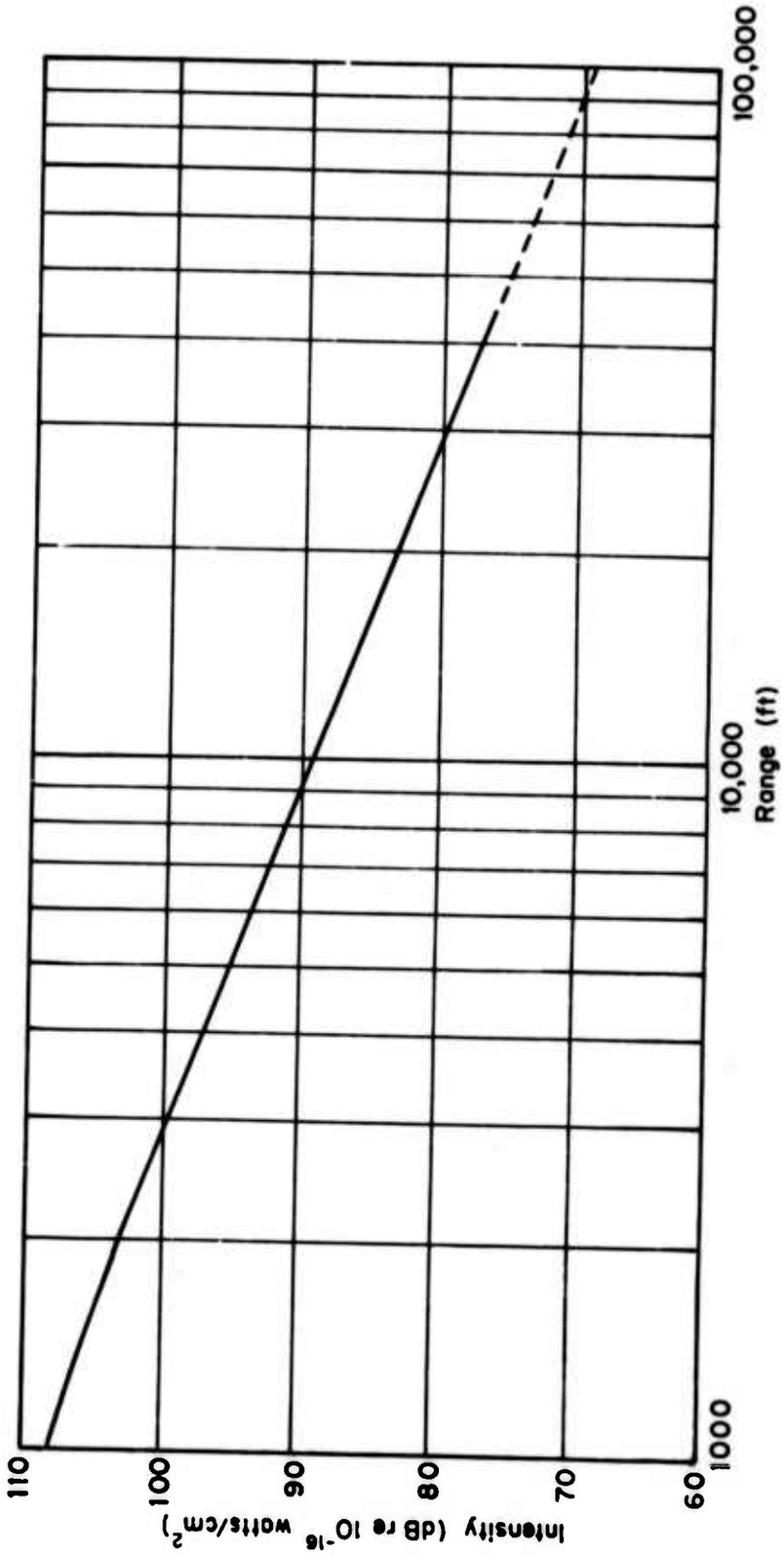

Fig. 8—Intensity variation with range (Case 2)

Case 3

The meteorological conditions in this case are shown below.

Altitude (ft)	Sound Velocity (ft/sec)	W_N (ft/sec)	W_E (ft/sec)
0	1100	0	0
2000	1095	0	40

It is seen that the gradient of sound velocity with altitude is negative, while the gradient of W_E with altitude is positive. With the introduction of wind the ray and intensity variations are no longer independent of azimuth. In Fig. 9 plots are shown of the sum of the sound velocity v and w_x for upwind and downwind propagation. It is seen that the gradient of $v + w_x$ is positive for downwind propagation and negative in the upwind case. Thus the resulting ray pattern shown in Fig. 10 is concave toward the earth in the right half plane and concave upward in the left half plane. In Fig. 11 the variation in intensity with distance for easterly or downwind propagation is shown to differ very little from an inverse-square variation. This is also true in Fig. 12 out to a distance of 6963 ft, beyond which a shadow zone is formed, similar to that of Fig. 5.

In the downwind direction for which $v + w_x$ has a positive gradient there is the possibility of surface ducting similar to that described in Case 2. However, as before, any modification of the intensity variation would be at extremely long range.

Case 4

In the cases considered thus far, a single-layer atmosphere has been assumed with uniform gradients of both sound velocity and wind velocity with altitude. In the present case a two-layer atmosphere is postulated as specified below.

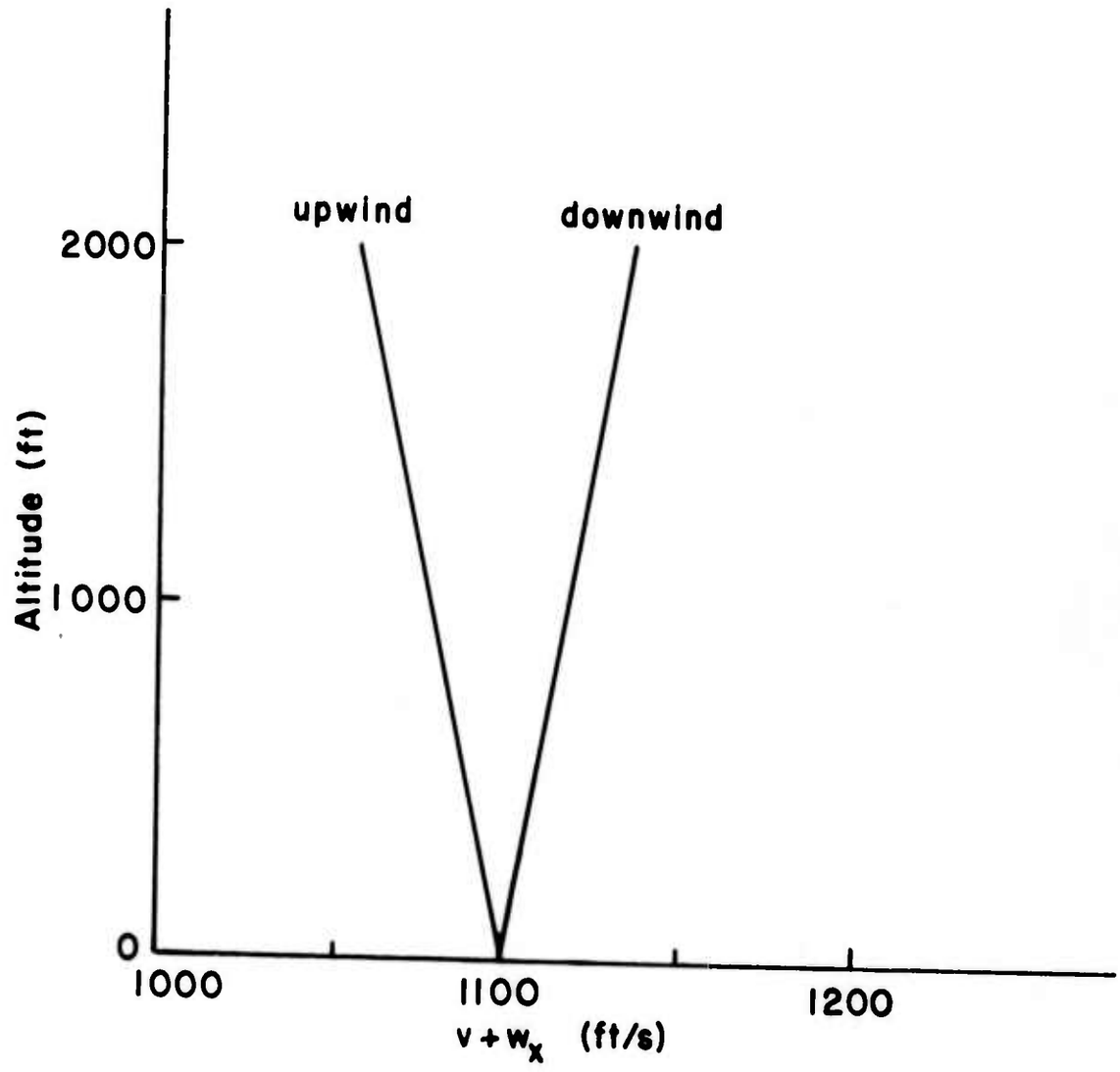

Fig. 9—Dependence of $v + w_x$ on altitude for upwind and downwind sound propagation (Case 3)

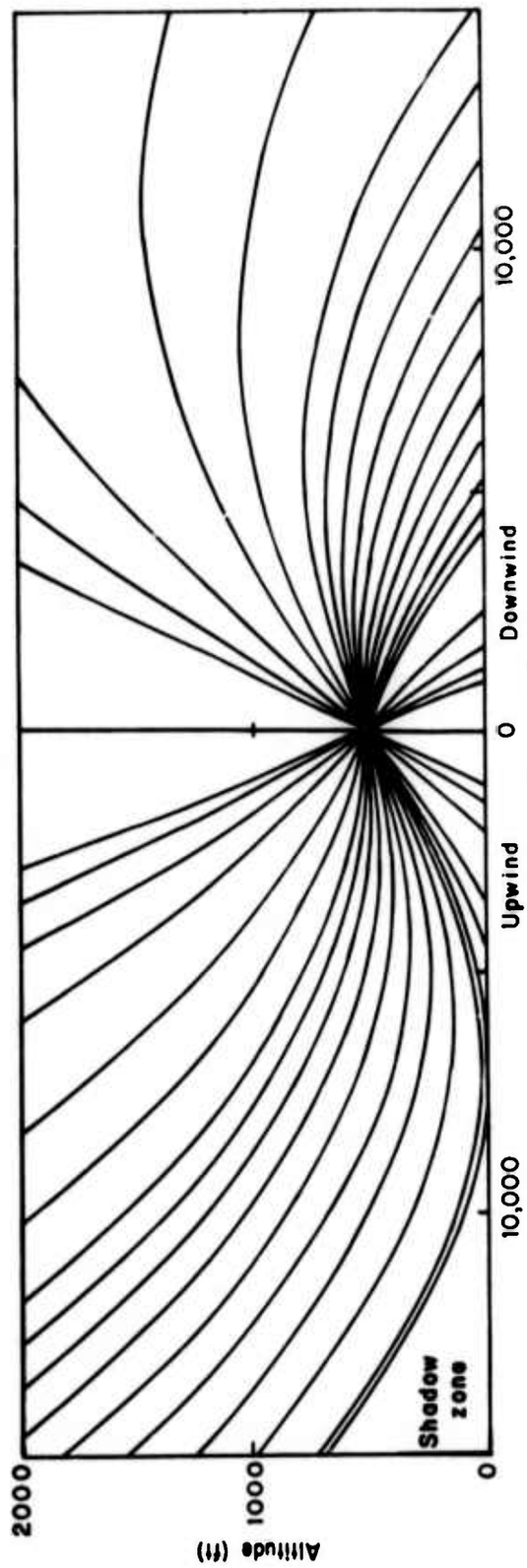

Fig. 10—Ray pattern (Case 3)

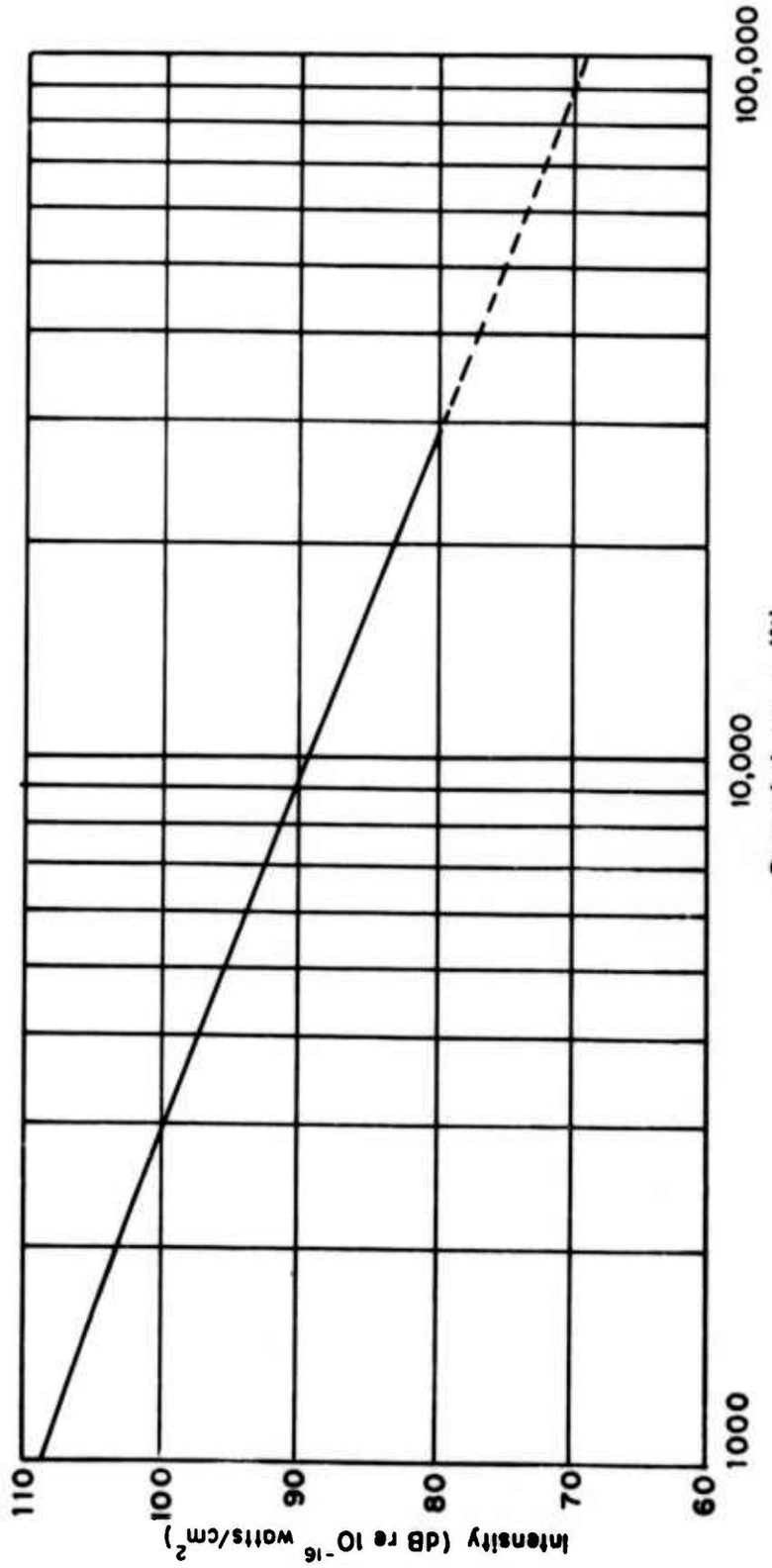

Fig. 11—Intensity variation with range in the downwind direction (Case 3)

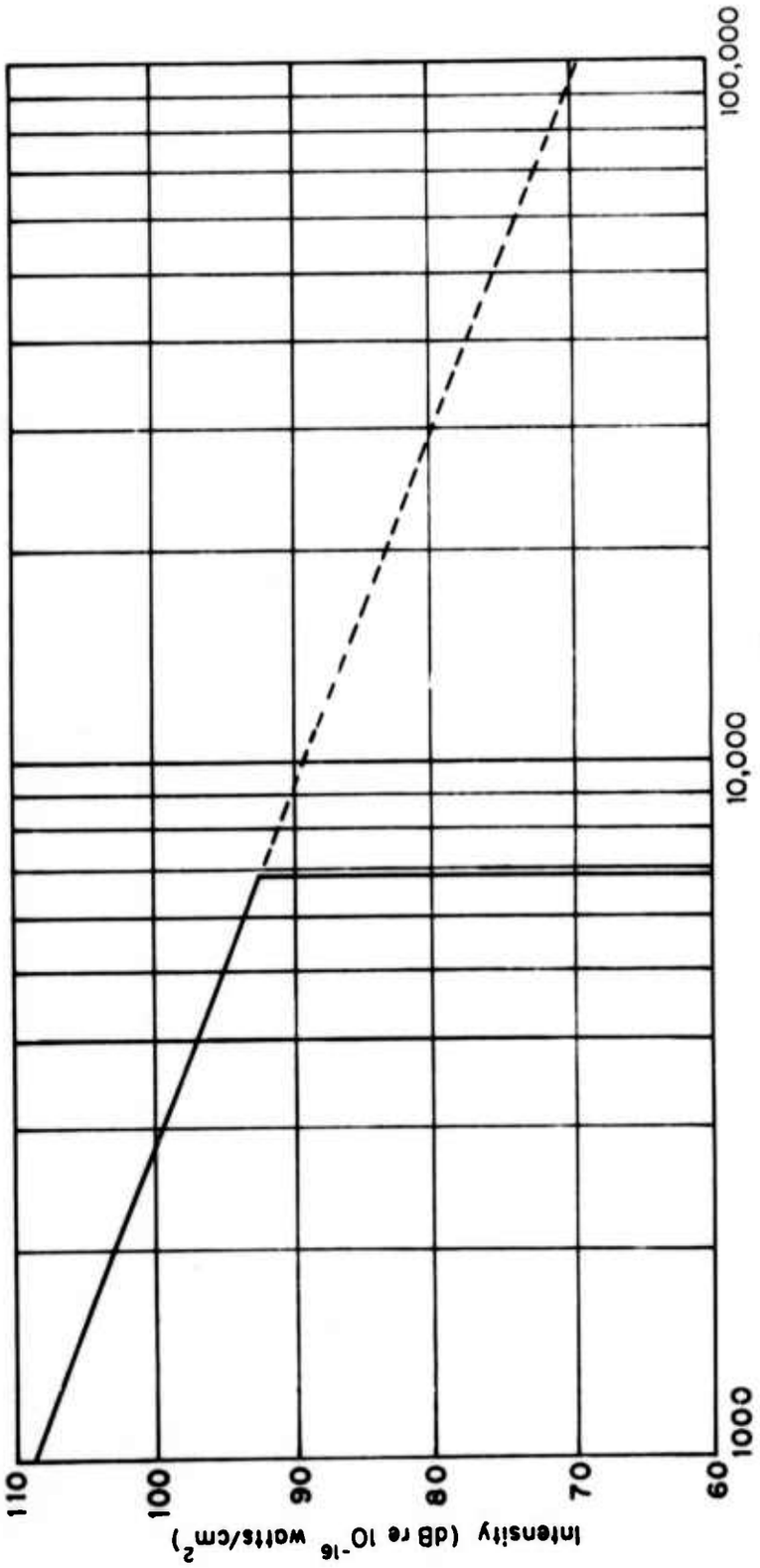

Fig. 12—Intensity variation with range in the upwind direction (Case 3)

Altitude (ft)	Sound Velocity (ft/sec)	W_N (ft/sec)	W_E (ft/sec)
0	1100.0	0	0
1000	1097.5	0	20
2000	1095.0	0	60

If the initial wave normal is in an eastward direction, then the x axis is also to the east and w_x is equal to W_E. Figure 13 shows that $v + w_x$ has a gradient of 17.5 ft/sec per 1000 ft between ground level and 1000 ft, while from 1000 to 2000 ft, this gradient increases to 37.5 ft/sec per 1000 ft.

The resulting ray pattern shown in Fig. 14 for eastward propagation again shows that for the positive gradient of $v + w_x$ the rays are concave toward the earth. However, as the initial wave normal increases from -25 deg to +7.21 deg the ground range of the corresponding rays increases from 1057 to 19,361 ft.

At 7.21 deg elevation the resulting ray is tangent to the boundary between the two atmospheric layers assumed and for elevation angles greater than 7.21 deg the ray spends part of its time in the upper layer where its curvature is greater due to the higher gradient of $v + w_x$. Thus for angles between 7.21 and 8.95 deg the ground range actually decreases from 19,361 to 16,458 ft. Finally, for elevation angles from 8.95 up to 16.34 deg the range again increases from 16,458 to 21,184 ft. At the latter elevation angle the ray reaches the maximum altitude for which meteorological data are given, and rays corresponding to higher elevation angles are terminated at the 2000-ft level.

An examination of the rays with elevation angles between 7.21 and 8.95 deg where ground range is decreasing shows that they form an envelope or caustic curve which starts at the maximum of the 7.21-deg curve (1000 ft altitude and 8036 ft downrange) and terminates at ground level 16,458 ft downrange. At any point on this caustic curve the value of the derivative $dr/d\Theta_o$ in Eq. (113) vanishes so that this line becomes a locus of infinite intensity. Actually such a conclusion goes beyond the validity of ray theory and in order to determine

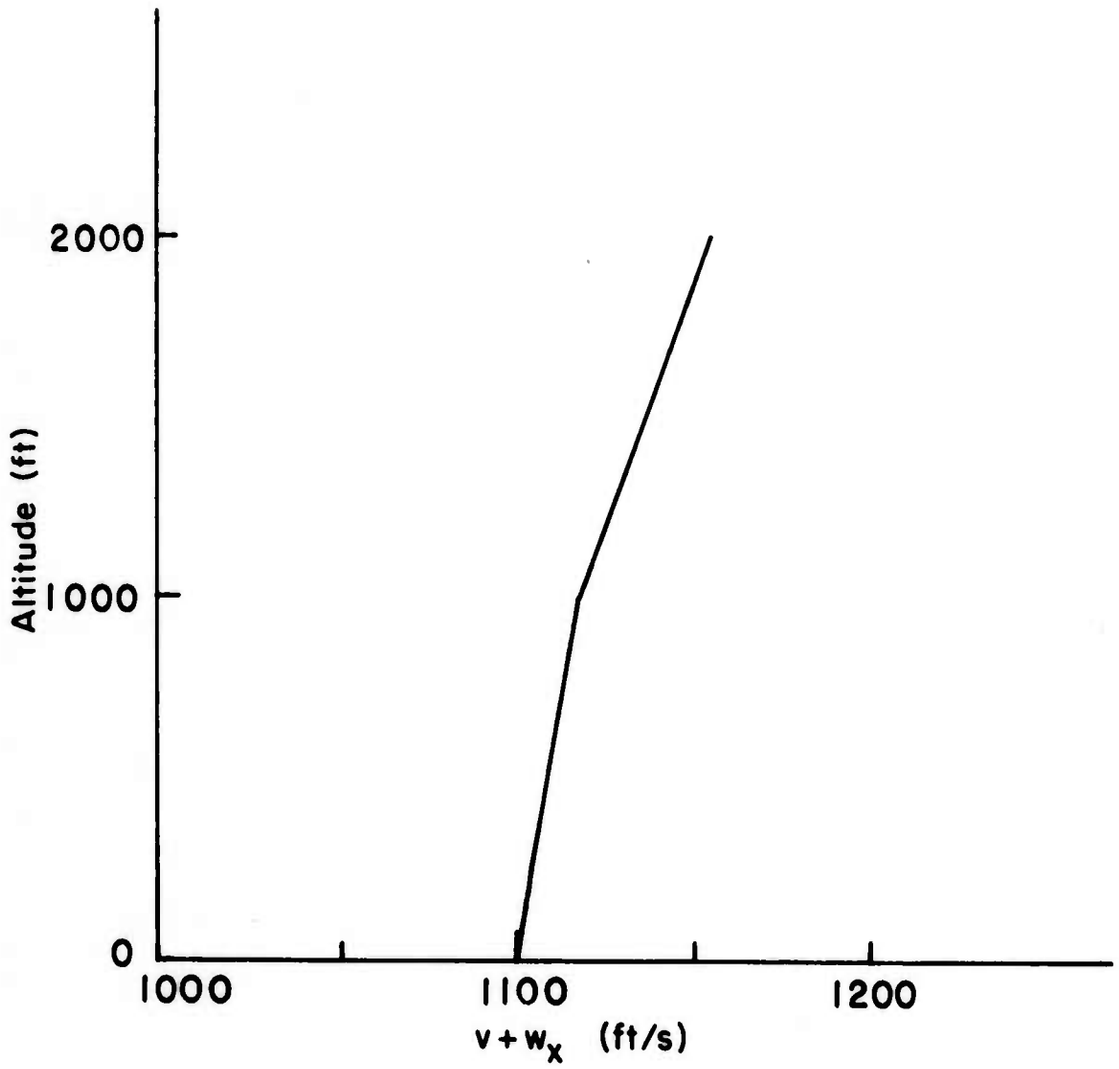

Fig. 13—Dependence of $v + w_x$ on altitude (Case 4)

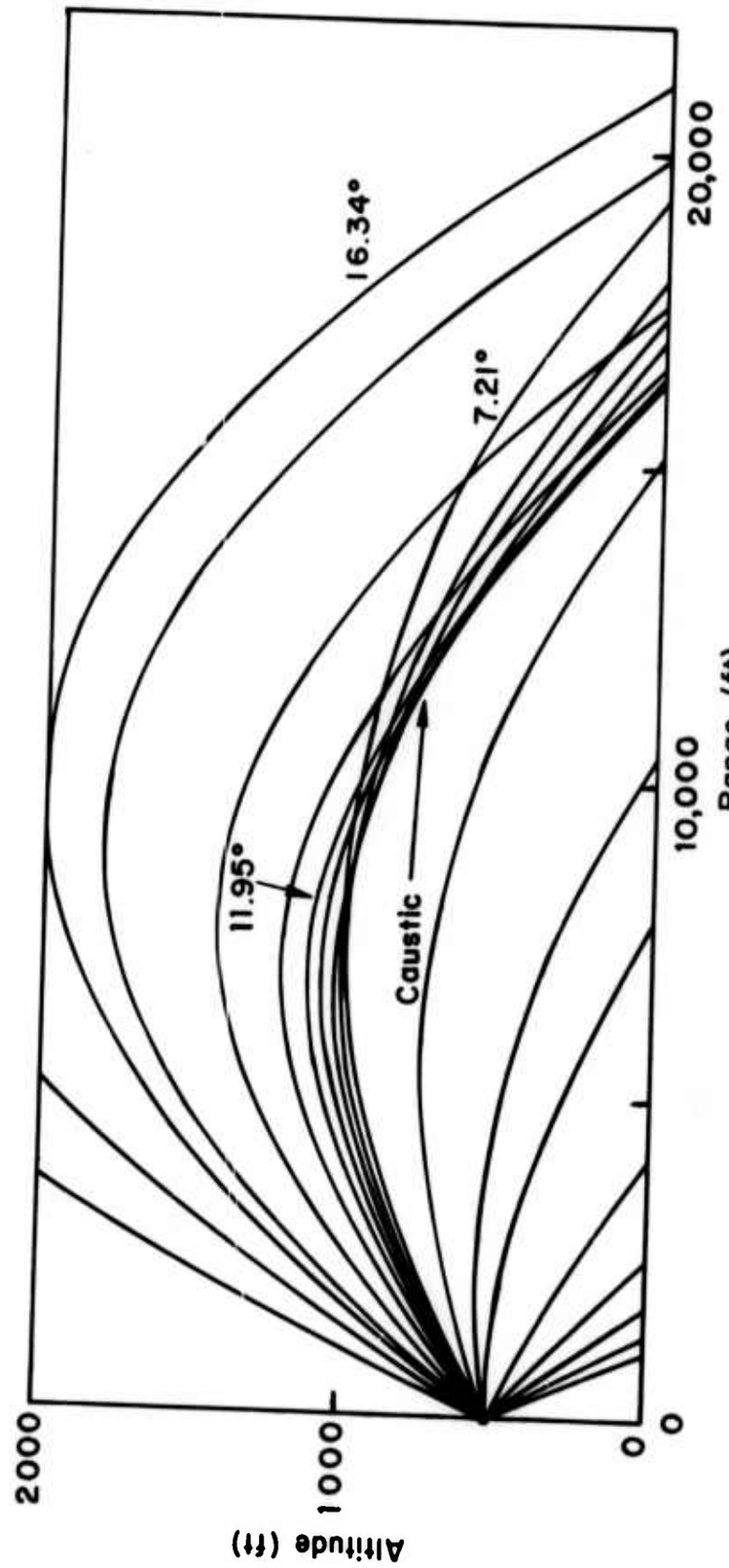

Fig. 14—Ray pattern (Case 4)

the intensity close to such a caustic curve it would be necessary to consider the diffraction effects associated with a wave solution to this problem. In Fig. 15 the intensity variation with distance based on the ray theory is shown for the above case. The arrows along the curves indicate the direction of increasing initial elevation angle while critical values of the elevation angle are indicated along the curve. Actually the curve has been extended to an elevation angle of 40.5 deg by assuming the same gradient above 2000 ft as exists between 1000 and 2000 ft.

It is seen that for ground ranges out to 16,458 ft there is a single ray reaching each point and the intensity has an inverse-square-law variation. For ranges greater than 19,361 ft there is also only a single arrival but the intensity decreases at a rate faster than the inverse square and drops below the curve for a homogeneous atmosphere at a range of about 26,000 ft. In the range interval between 16,458 and 19,361 ft there are three rays which reach any point on the ground corresponding to the three branches of the intensity curve. If it is assumed that the pressure variations in the sound wave are random, then the resultant intensity can be expressed as

$$I = I_1 + 10 \log_{10}\left[1 + 10^{\frac{I_2 - I_1}{10}} + 10^{\frac{I_3 - I_1}{10}}\right] \qquad (114)$$

where I_1, I_2, and I_3 are the intensities in dB corresponding to the three branches of the intensity curve for a given range while I is the resultant intensity in dB. Figure 16 is an enlargement of the multiple arrival region of Fig. 15 showing the three component curves and the resultant intensity curve computed from Eq. (114). The cusp in this curve occurs where the caustic curve discussed earlier intersects the ground.

As indicated previously, ray theory is not valid in the vicinity of a caustic and if a wave theory solution were utilized in this region the resultant intensity peak would probably not exceed 93 dB or about 8 db above the inverse-square-law intensity for a homogeneous

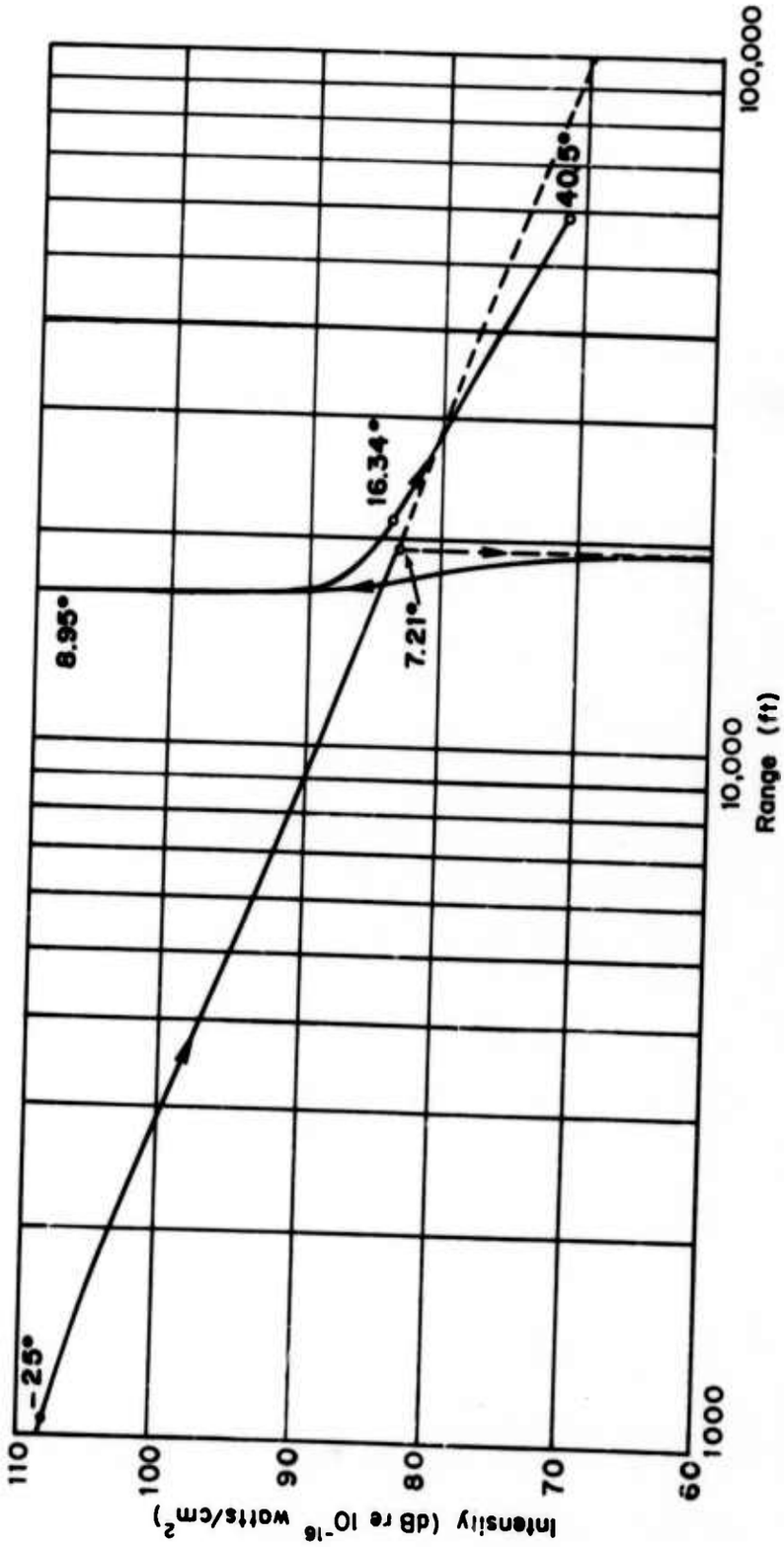

Fig. 15—Intensity variation with range (Case 4)

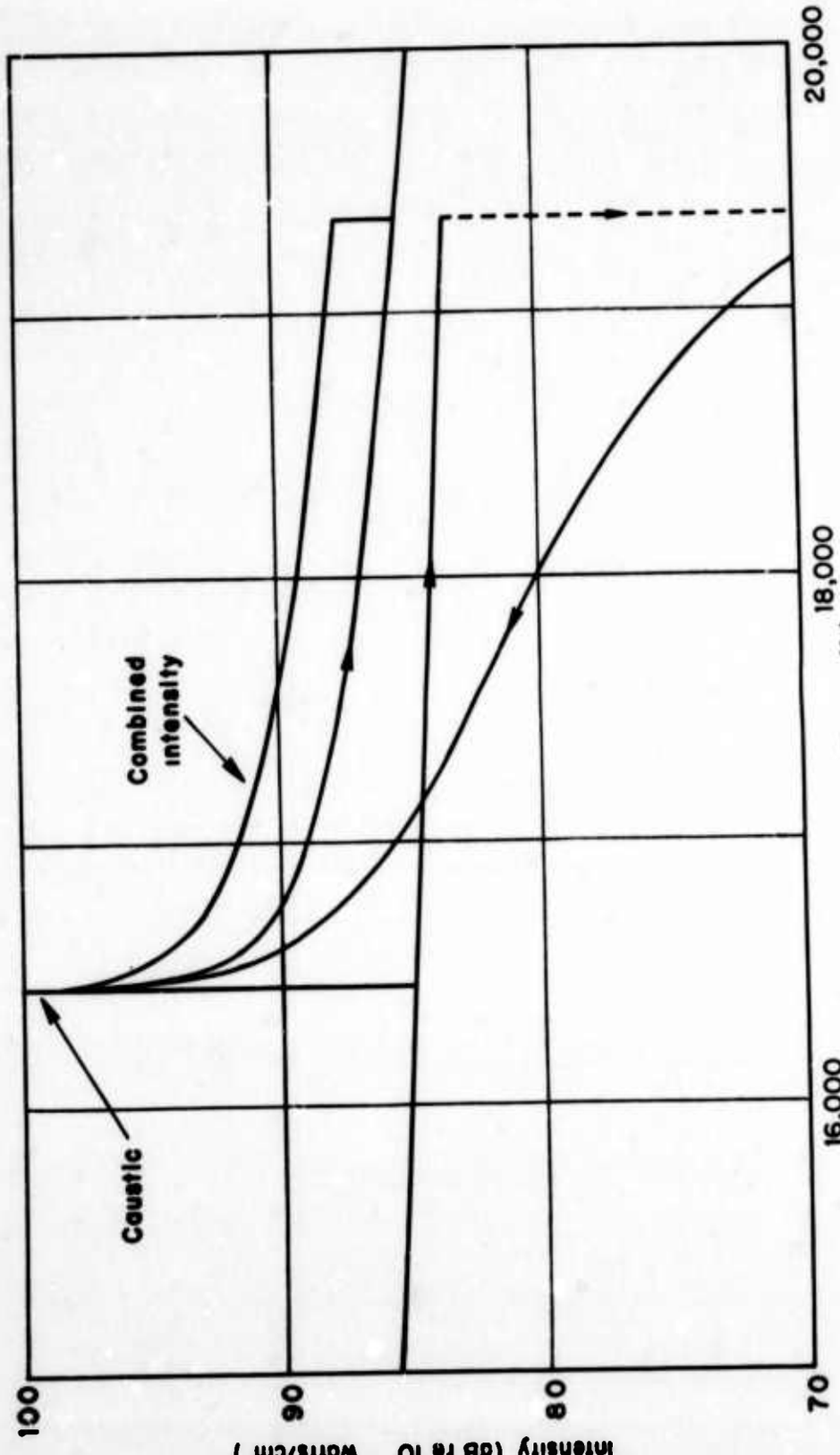

Fig. 16—Intensity variation in the vicinity of the caustic (Case 4)

atmosphere. Similarly the step change in intensity at the longer range end of the multiple arrival region would also be smoothed out by a wave solution in this region. However, this type of atmospheric profile does result in appreciable deviations from an inverse-square-law drop-off of intensity even in the absence of atmospheric attenuation.

Case 5

This case is also a two-layer atmosphere with characteristics as specified below.

Altitude (ft)	Sound Velocity (ft/sec)	W_N (ft/sec)	W_E (ft/sec)
0	1100.0	0	0
1000	1097.5	0	20
2000	1095.0	0	30

If as in Case 4 the initial wave normal azimuth is east then Fig. 17 represents the plot of $v + w_x$ for this azimuth of propagation. A comparison of this figure with the corresponding one for Case 4 shows that up to 1000 ft the gradients are identical. However, above 2000 ft the gradient of $v + w_x$ decreases to a value of 7.5 ft/sec per 1000 ft.

The resulting ray pattern for a source at 500-ft altitude is shown in Fig. 18, and as would be expected from the positive gradients of Fig. 17, the rays are concave toward the ground. However, the curvature of those portions of the rays above 1000 ft is considerably less than that below 1000 ft due to decrease in the gradient of $v + w_x$ at the higher altitude. As a result, the ground range of the rays increases monotonically with initial inclination angle and there is no region of multiple arrival as in Case 4.

In Fig. 19 the corresponding variation of intensity with range shows an inverse-square-law variation out to 19,361 ft. This range as in Case 4 corresponds to the ray which is tangent to the 1000 ft altitude boundary between the two layers of the assumed atmosphere.

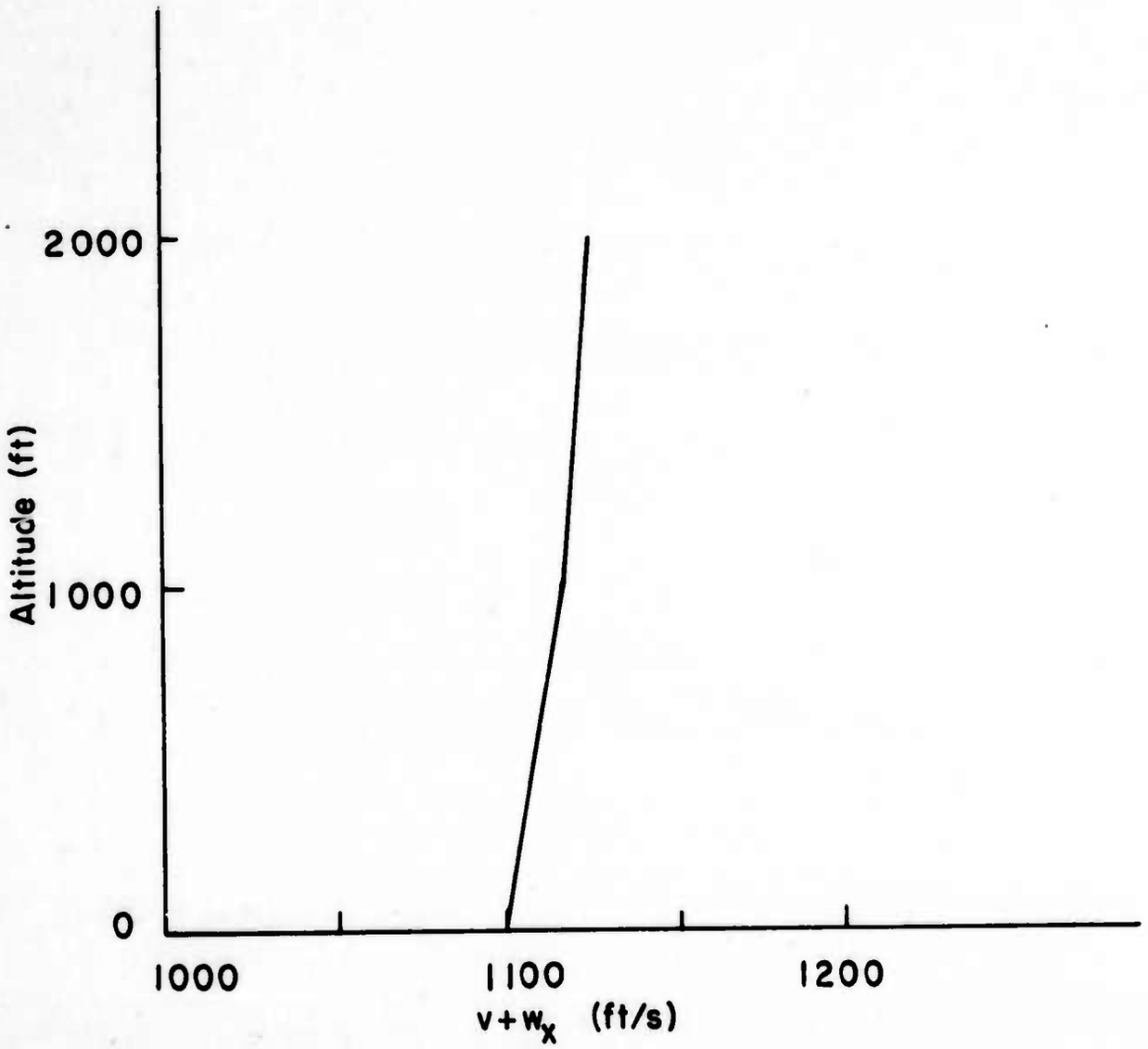

Fig. 17—Dependence of $v + w_x$ on altitude (Case 5)

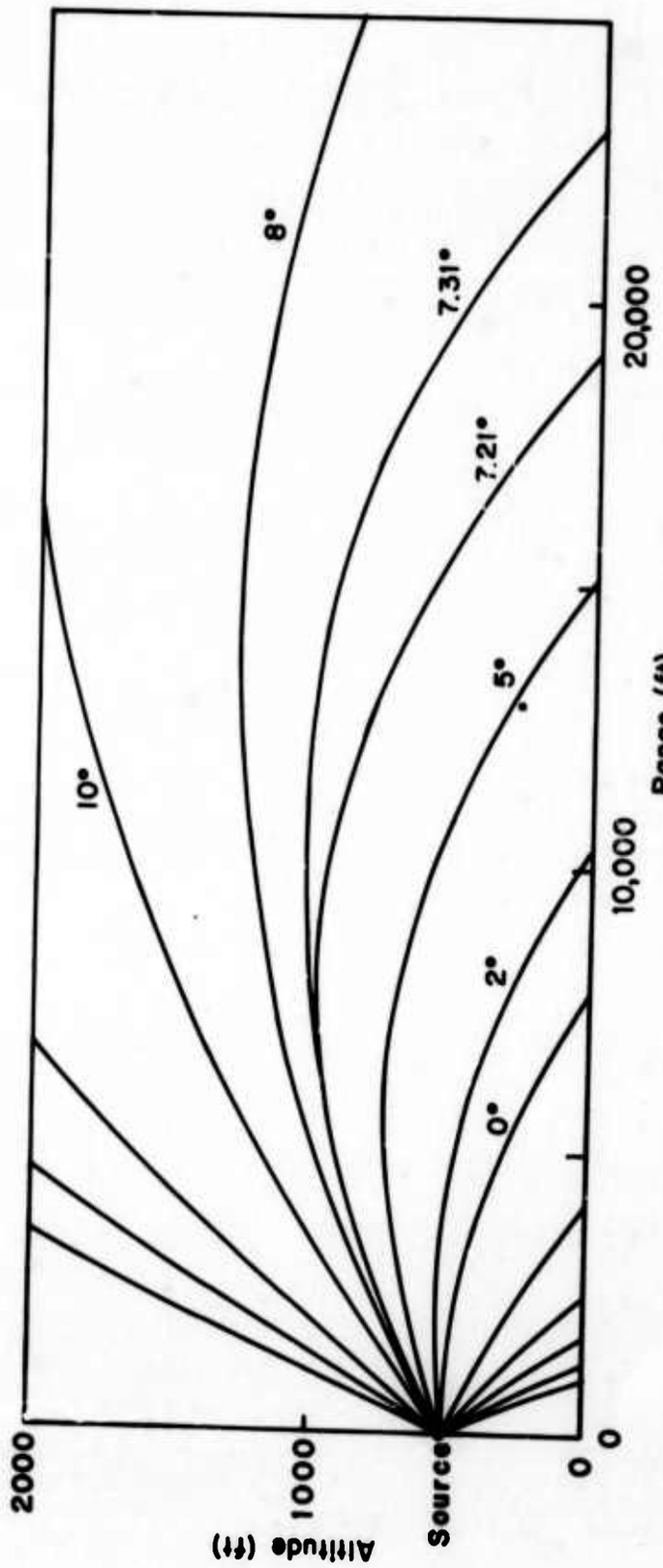

Fig. 18—Ray pattern (Case 5)

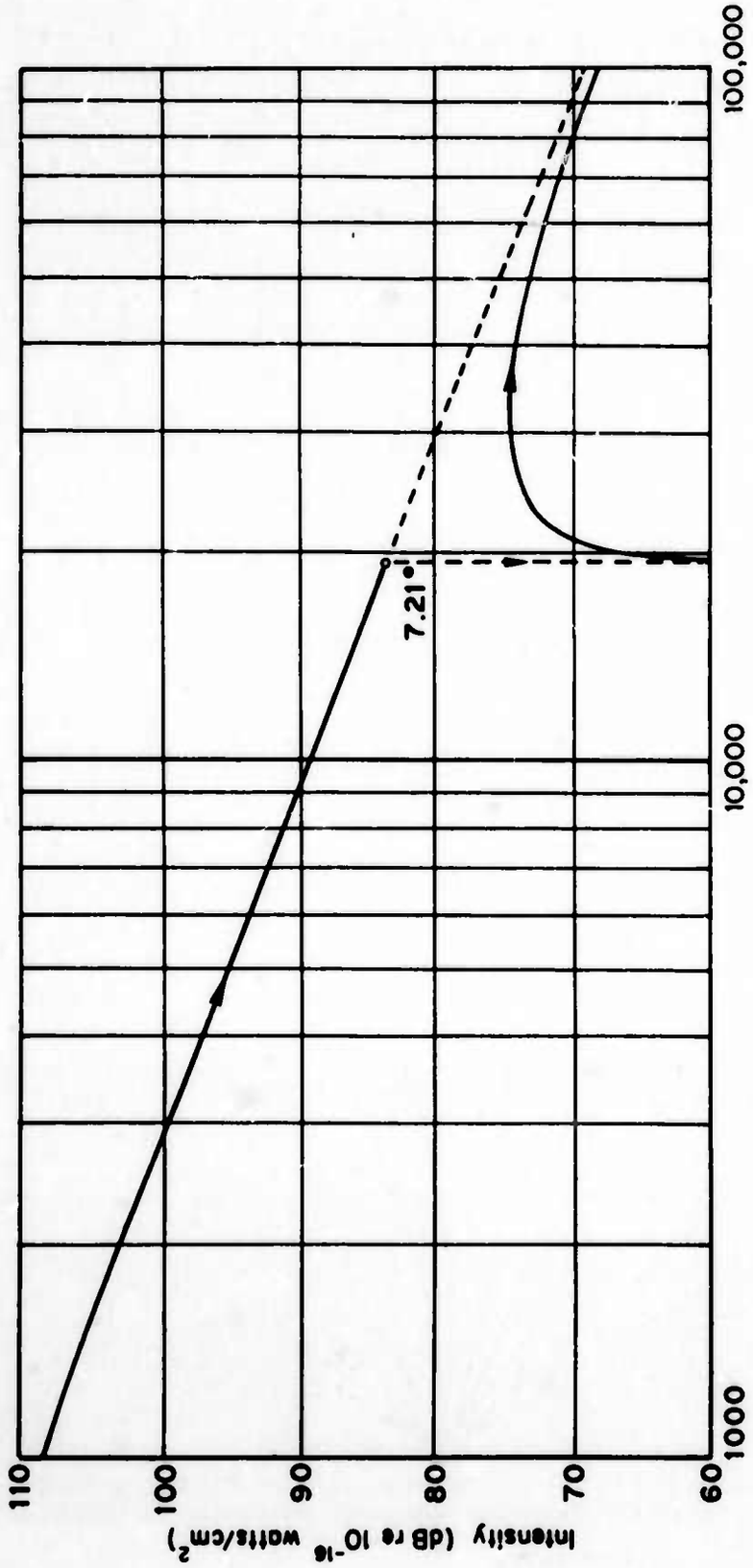

Fig. 19—Intensity variation with range (Case 5)

Beyond this critical range, the intensity drops abruptly to zero, after which it increases rapidly to a maximum of about 74.5 dB at 32,500 ft. It then decreases again, always lying below the homogeneous atmosphere curve. This type of intensity variation can be explained as follows. As long as the initial elevation angle of the ray is low enough that the ray remains below the 1000-ft level the divergence of the rays results in the inverse-square-law intensity variation observed previously for a constant gradient of $v + w_x$. However, when the initial elevation angle reaches a value at which the ray begins to penetrate the upper layer with a lower gradient of $v + w_x$, there is a discontinuity in the rate of change of ground range with elevation angle. As a result the value of $dr/d\Theta_o$ in Eq. (113) becomes infinite and a zero intensity results immediately beyond the critical range of 19,361 ft. As the elevation angle continues to increase the value of $dr/d\Theta_o$ decreases and the intensity increases rapidly. However, as the elevation angle increases farther and more and more of the path lies in the upper layer, the intensity variation begins to approach the inverse-square law, corresponding again to a constant gradient of $v + w_x$. It should also be noted that in actual practice these apparent discontinuities would be somewhat smoothed out by diffraction effects and also by the fact that the change in gradient at the 1000-ft level would probably not be discontinuous as assumed here.

In Fig. 20 the intensity variations for Cases 4 and 5 are plotted on the same graph for comparison. It is seen that for these two cases the meteorological conditions up to 1000 ft altitude are identical. However, as a result of differences in conditions in the layer between 1000 and 2000 ft there are differences in intensity of as much as 10 dB between the two cases at ranges in the vicinity of 22,000 ft.

Case 6

The assumed meteorological conditions for this case are shown below.

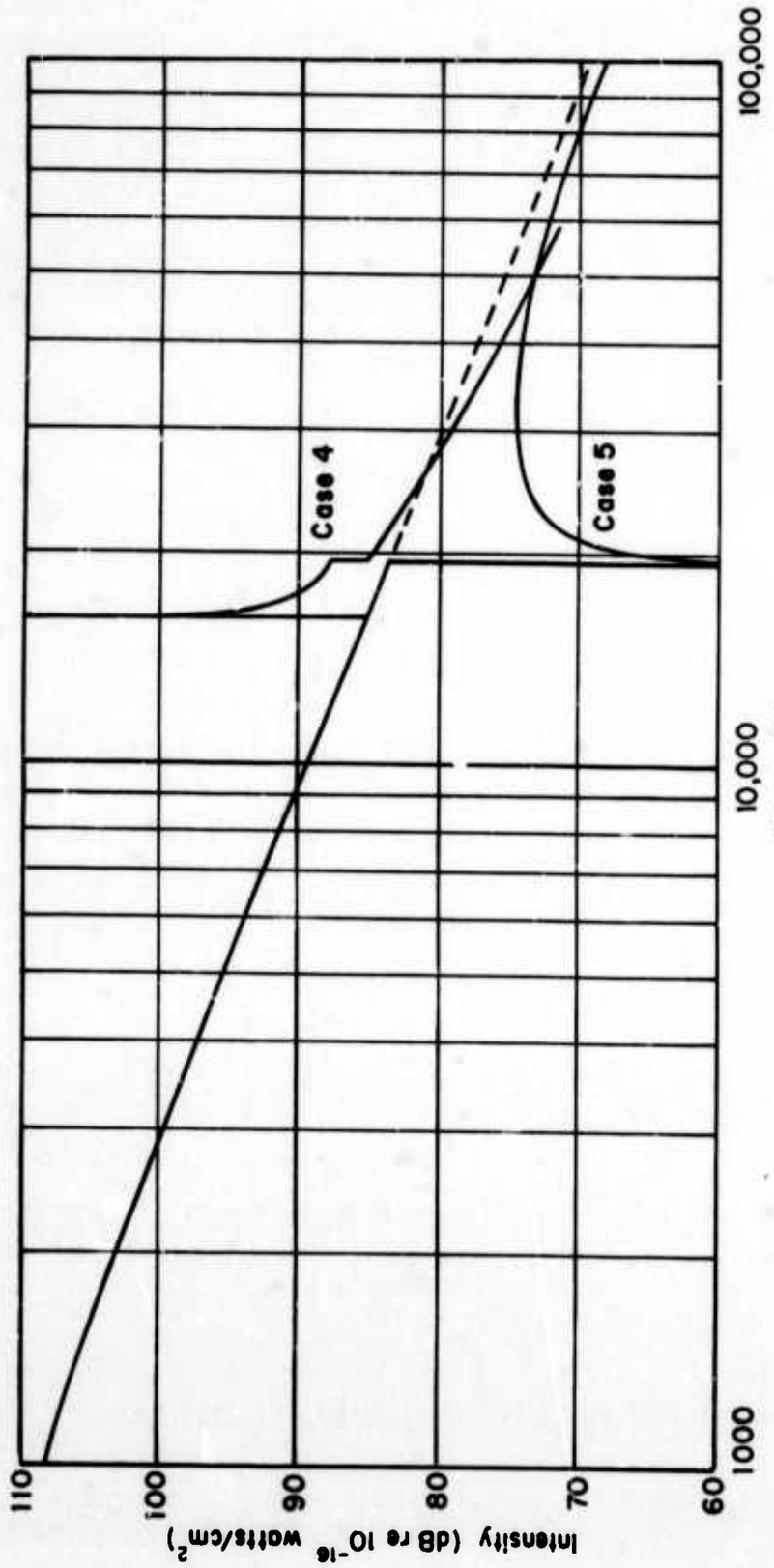

Fig. 20—Intensity comparison between Cases 4 and 5

Altitude (ft)	Sound Velocity (ft/sec)	W_N (ft/sec)	W_E (ft/sec)
0	1100.0	0	0
1000	1097.5	0	-10
2000	1095.0	0	30
3000	1092.5	0	20

If again the initial wave normal azimuth is eastward, then Fig. 21 represents the plot of $v + w_x$ for this azimuth of propagation. It is seen that from 0 to 1000 ft there is a negative gradient of $v + w_x$ of 12.5 ft/sec per 1000 ft, while from 1000 to 2000 ft the gradient reverses and has a value of 37.5 ft/sec per 1000 ft, and finally above 2000 ft the gradient is again negative with a value of 12.5 ft/sec per 1000 ft.

Figure 22 shows the resulting ray pattern emanating from the source. It is seen that in the regions of negative gradient of $v + w_x$ the rays are concave upward while in regions of positive gradient they are concave downward. For initial values of wave normal elevation less than -6.1 deg the value of C is greater than 1100 ft/sec, the value of $v + w_x$ at ground level, and the corresponding rays all reach the ground. The ray having an initial wave normal elevation of -6.1 deg has a value of C equal to 1100 ft/sec and is tangent to the ground at a range of 9192 ft, after which it rises to a maximum altitude of 1333 ft, where the value of $v + w_x$ again equals 1100 ft/sec. For elevation angles between -6.1 deg and +6.1 deg the values of C are less than 1100 ft/sec and a given ray is bounded between the two altitudes at which $v + w_x$ equals the value of C for that ray. When the elevation angle equals +6.1 deg the ray is tangent to the ground at a range of 25,871 ft after first reaching a maximum altitude of 1333 ft. As the initial elevation angle increases from 6.1 to 13.51 deg the values of C lie between 1100 and 1125 ft/sec. The corresponding rays rise to a maximum altitude at which $v + w_x$ equal C after which they descend to ground level. As the elevation angle increases from 6.1 to 9.7 deg the ground range decreases from 25,871 to 20,415 ft while from 9.7 to 13.51 deg the range increases again to 21,617 ft. For elevation angles in excess of 13.51 deg the value of C is greater than any of the specified values of $v + w_x$ and the

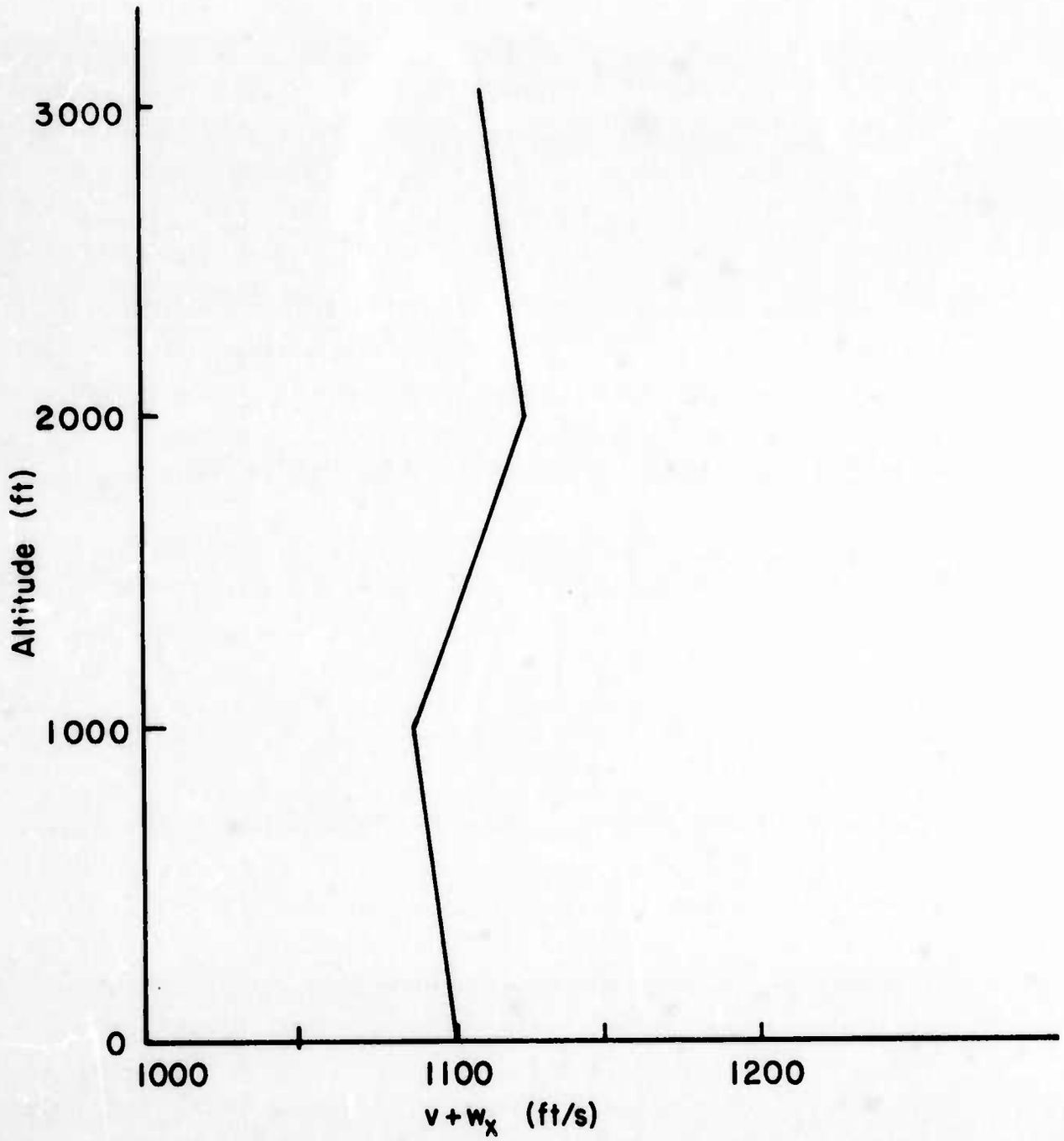

Fig. 21—Dependence of $v + w_x$ on altitude (Case 6)

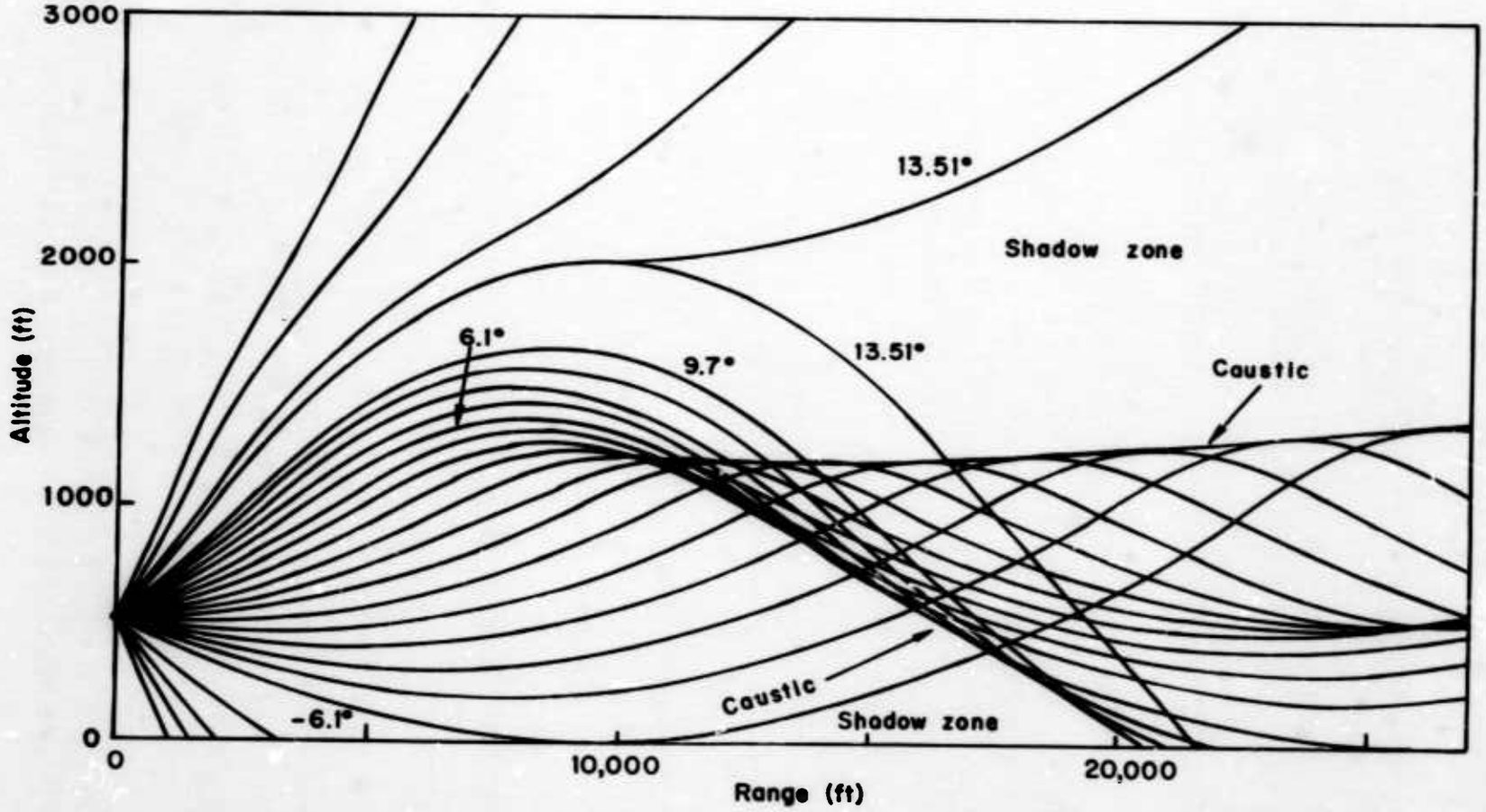

Fig. 22—Ray pattern (Case 6)

rays do not reach a maximum altitude and thus do not return to ground level.

This example demonstrates the phenomenon of ducting since all of the energy radiated between elevation angles of -6.1 deg and +6.1 deg is confined between the ground and an altitude of 1133 ft. The actual upper bound of the duct is the nearly horizontal caustic curve shown in the figure. A second caustic curve is formed by the rays having initial elevation angles between 6.21 and 9.7 deg. This caustic is also very nearly a straight line and intersects the ground at a range of 20,415 ft. There are two shadow zones associated with this ray pattern. The first is bounded by the rising portion of the ray tangent to the ground at 9192 ft, the second caustic curve, and the ground surface. The other shadow zone is entirely above ground level and is bounded by the two branches of the 13.51 deg ray which splits at 3000 ft and the horizontal caustic which is the upper bound of the duct.

In Fig. 23 the variation of intensity with ground range is shown. It is seen that out to a range of 9192 ft the intensity drops off in accordance with the inverse-square law. Between 9192 and 20,415 ft the intensity drops to zero while from 20,415 to 25,871 ft there is a second zone of audibility with an infinite intensity at 20,415 ft where the caustic curve intersects the ground, and a region of double arrival between 20,415 and 21,617 ft. As in Case 4 diffraction effects would round off the infinite intensity cusp; however, it appears likely that in this second region of audibility the intensity might be as much as 6 dB above the curve for a homogeneous atmosphere.

METEOROLOGICAL DATA

To investigate the nature of sound transmission under arctic weather conditions, three representative sets of meteorological data were selected from Ref. 8. The information relevant to sound propagation is shown in Tables 1 through 3.

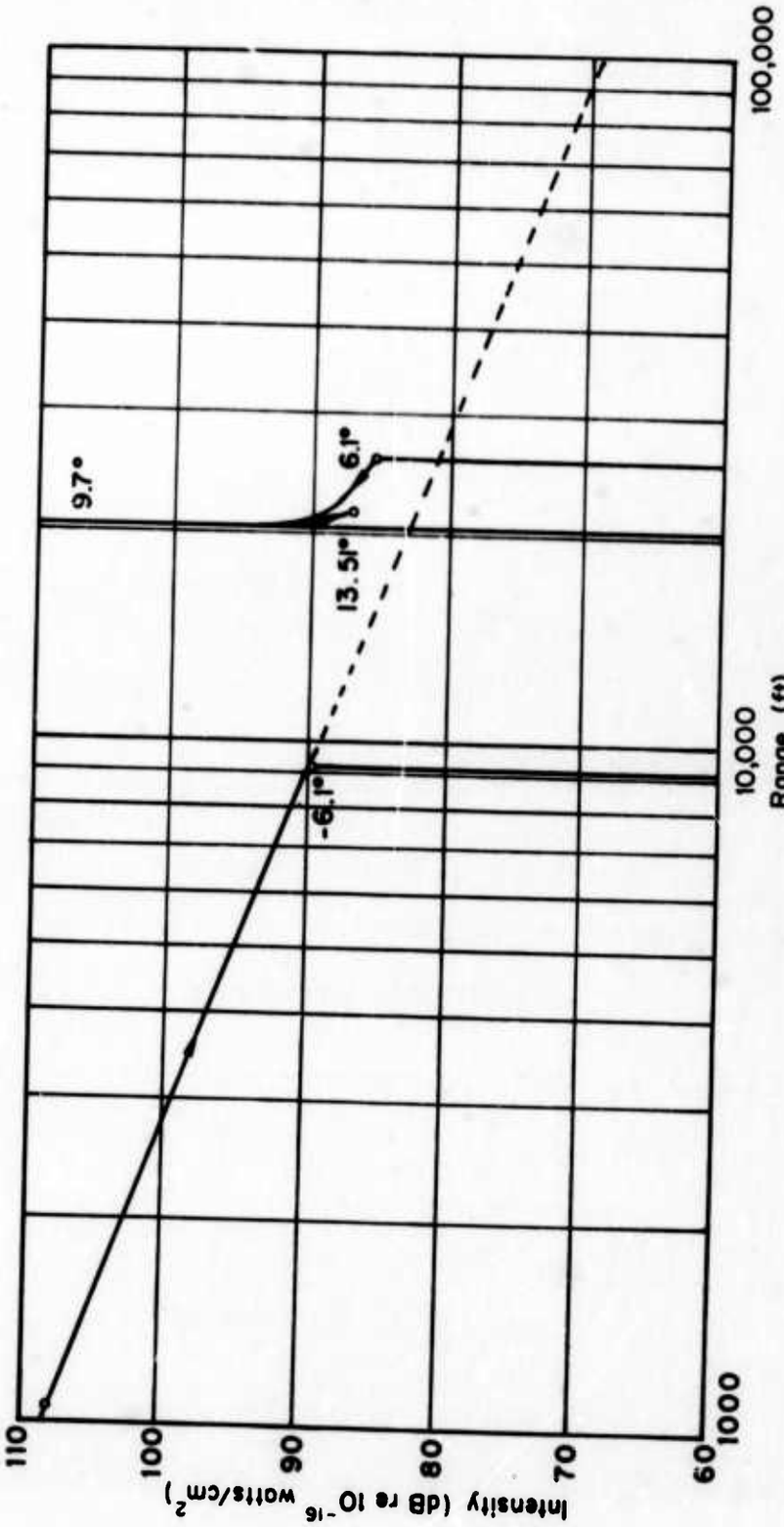

Fig. 23—Intensity variation with range (Case 6)

Table 1

PROFILE 1

Level	Altitude (ft)	Sound Velocity (ft/sec)	W_E (ft/sec)	W_N (ft/sec)	Relative Humidity (%)
0	0	1010.8	15.7	8.9	30.0
1	492	1012.9	30.2	13.8	35.0
2	820	1015.0	37.1	13.8	40.0
3	984	1019.3	40.7	13.8	43.0
4	2133	1023.5	52.2	6.6	57.0
5	4265	1027.7	51.5	-0.7	53.0
6	6890	1025.6	49.2	0.0	41.0
7	9843	1020.3	49.2	0.0	28.0

Table 2

PROFILE 2

Level	Altitude (ft)	Sound Velocity (ft/sec)	W_E (ft/sec)	W_N (ft/sec)	Relative Humidity (%)
0	0	1050.7	3.0	2.6	93.0
1	328	1055.4	19.4	10.2	93.0
2	656	1060.3	29.5	8.9	93.0
3	1148	1067.0	34.4	3.3	93.0
4	2625	1069.0	32.8	0.0	93.0
5	9843	1044.5	32.8	0.0	90.0

Table 3

PROFILE 3

Level	Altitude (ft)	Sound Velocity (ft/sec)	W_E (ft/sec)	W_N (ft/sec)	Relative Humidity (%)
0	0	1099.0	36.7	13.1	79.0
1	656	1096.2	47.6	15.7	79.5
2	1640	1092.1	63.0	12.5	80.0
3	2953	1086.5	68.6	5.9	81.0
4	4265	1081.1	68.2	0.0	82.5
5	7874	1067.0	66.6	0.0	85.0
6	9843	1061.9	65.6	0.0	85.0

ARCTIC SOUND TRANSMISSION

In the following paragraphs, the variation of sound intensity as a function of ground range and azimuth of propagation is determined for each of the meteorological profiles given in Tables 1 through 3. In all of these cases a source power of 100 kW at an altitude of 500 ft is assumed.

Profile 1

In Fig. 24 plots of $v + w_x$ as a function of altitude are shown for Profile 1 at intervals of 30 deg in azimuth from 0 to 360 deg, where the azimuth angle is measured counterclockwise from east.

The variation of intensity as a function of ground range is shown in Fig. 25 for an azimuth angle of 0 deg. It is seen that out to a range of 11,500 ft the intensity has essentially an inverse-square-law decrease. Between 11,500 and 13,000 ft an increase occurs because of the increase in the gradient of $v + w_x$ at the 820-ft level. This effect is similar to that shown in Example 4 and results in a caustic which intersects the ground at about 11,750 ft range. The branch of the intensity curve between 12,000 and 34,000 ft range is due to the decrease in gradient at the 984-ft level and is similar to Example 5. Finally, the branch beyond 34,000 ft in range results from the decrease in gradient at the 2133-ft level.

As the azimuth angle increases, the gradient in the layer above 2133 ft becomes negative and the corresponding branch of the intensity curve disappears as shown in Fig. 26 since rays which go above this level are no longer refracted back to the ground. A further increase in azimuth results in a negative gradient above 980 ft so that the second branch of the intensity curve also disappears as shown in Fig. 27. For azimuth angles between 120 and 210 deg the gradient is completely negative and the intensity curve is similar to that shown for the upwind direction in Example 3 where a shadow zone is formed.

At an azimuth of 240 deg the shadow zone still exists, however, because of the positive gradient above 820 ft the value of $v + w_x$ above 3000 ft exceeds that at ground level, and it is possible to have

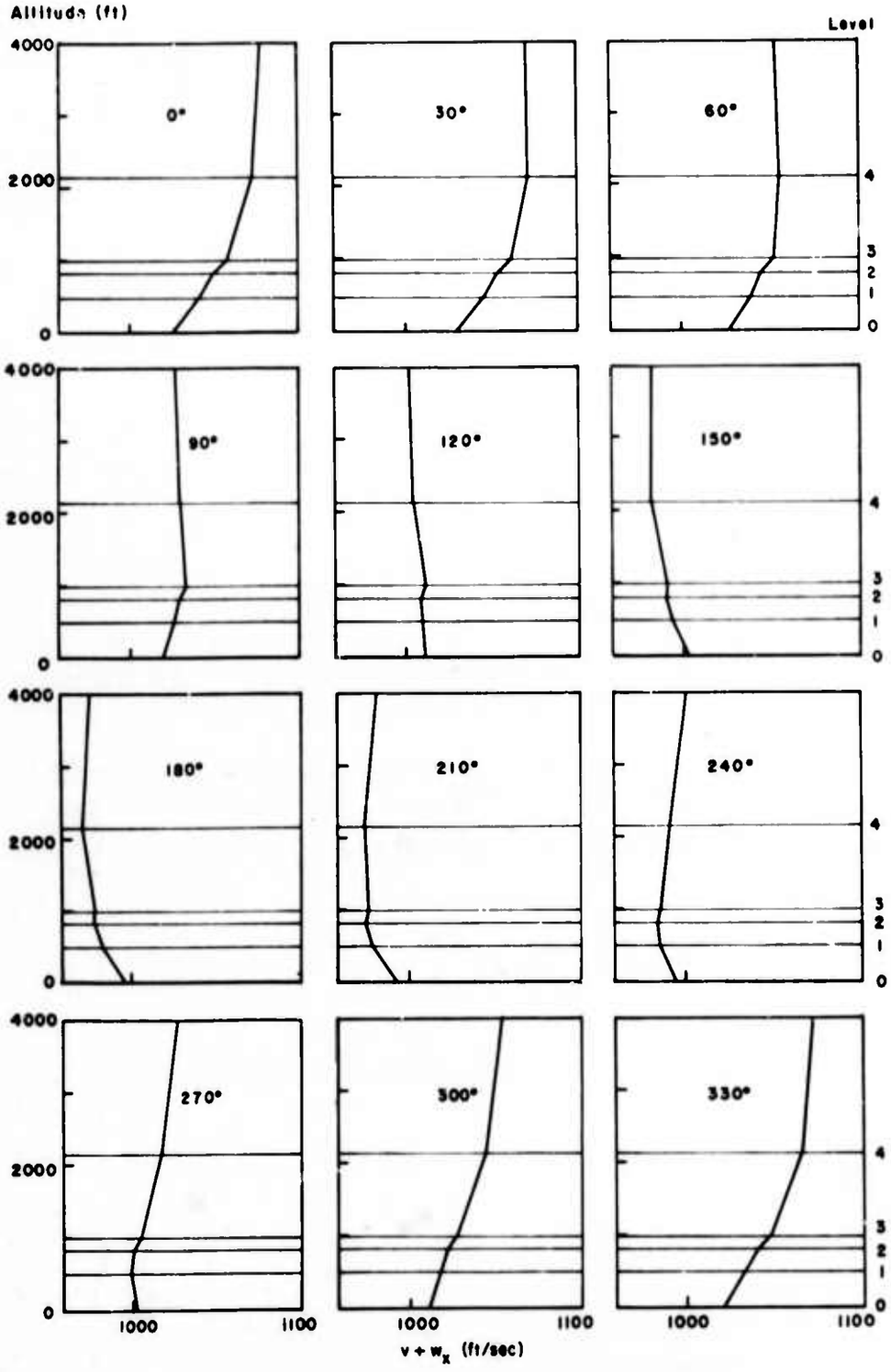

Fig. 24—Dependence of $v + w_x$ on altitude at 30° intervals in azimuth of propagation (Profile 1)

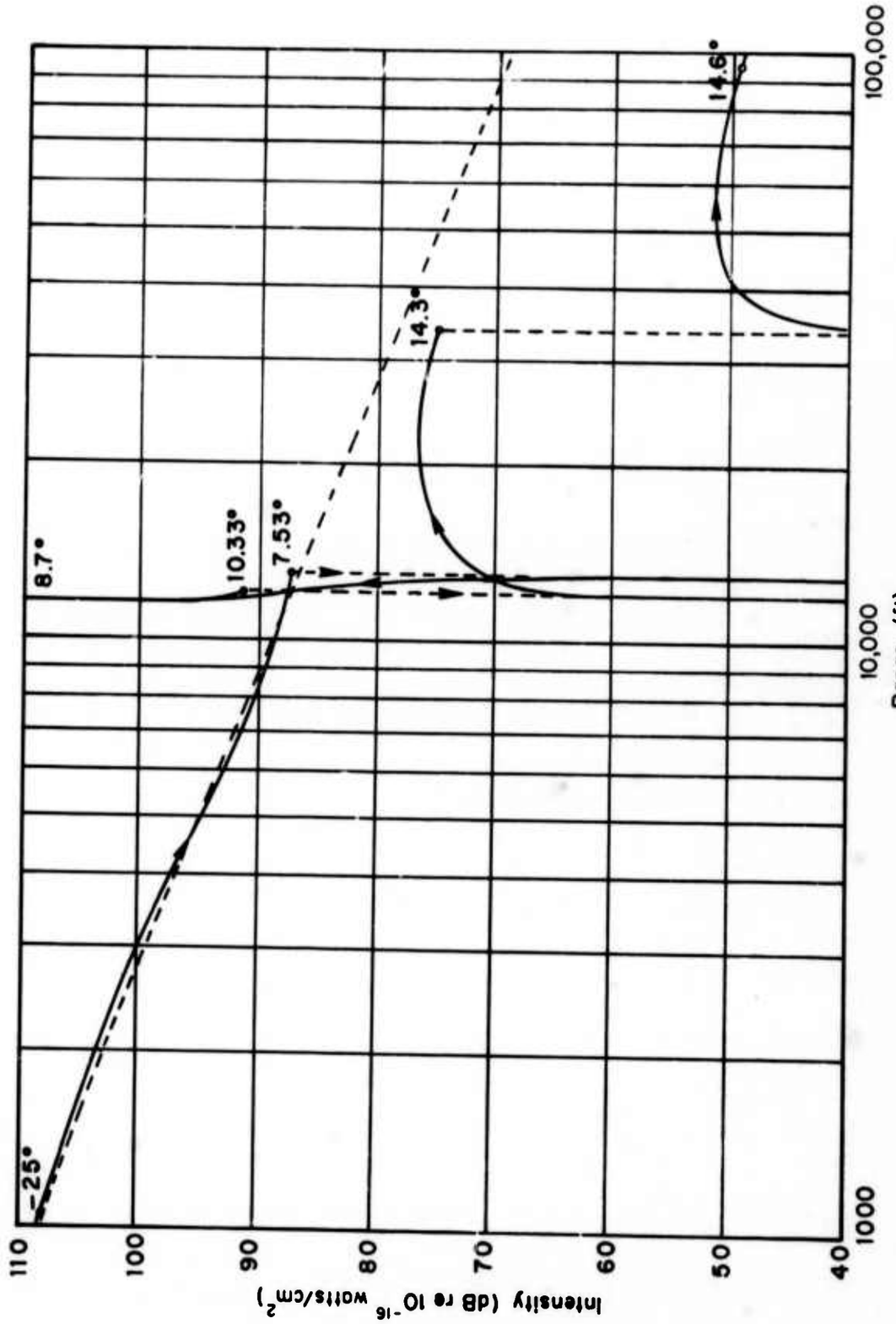

Fig. 25—Intensity variation with range at 0° azimuth (Profile 1)

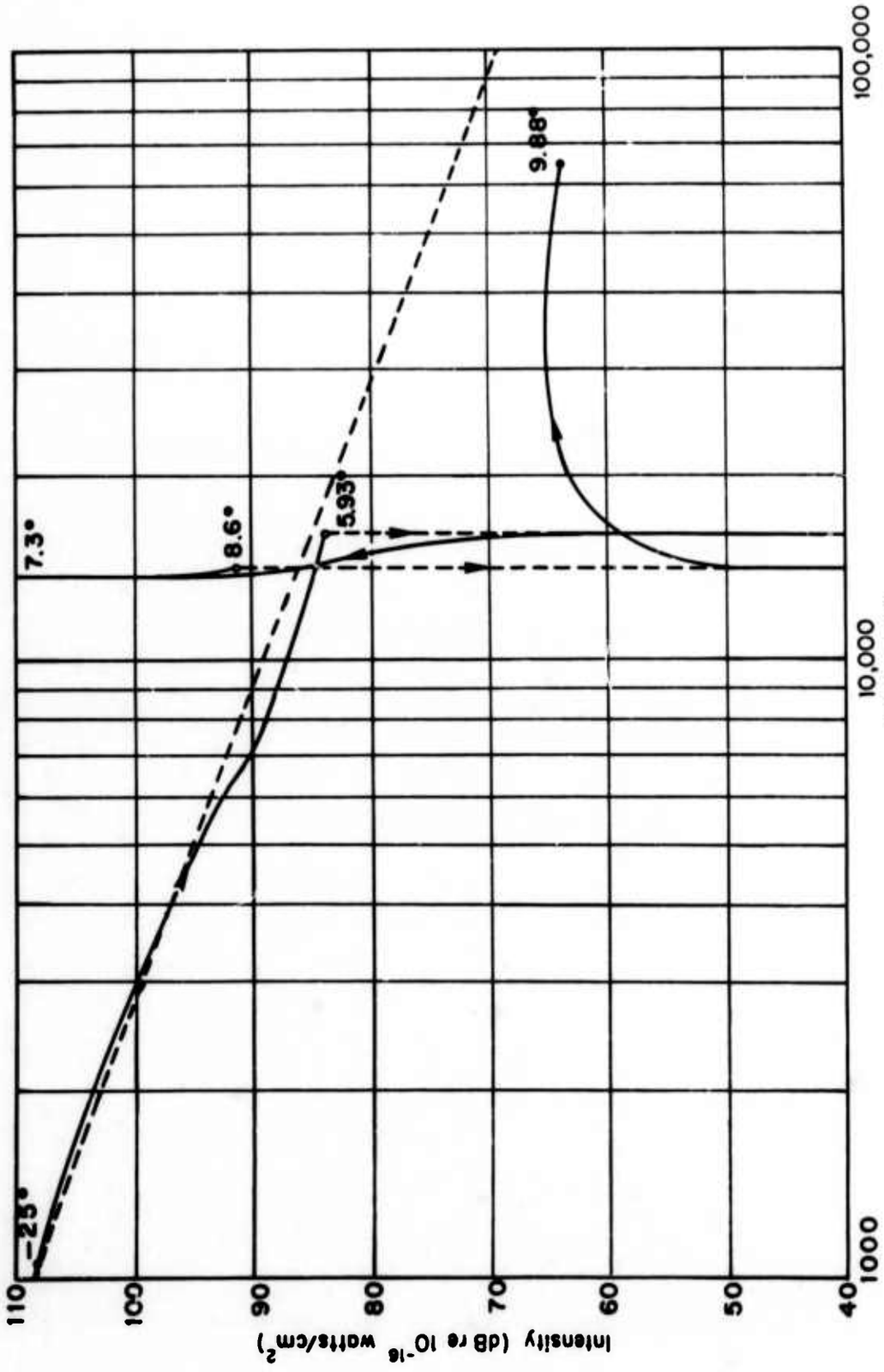

Fig. 26—Intensity variation with range at 60° azimuth (Profile 1)

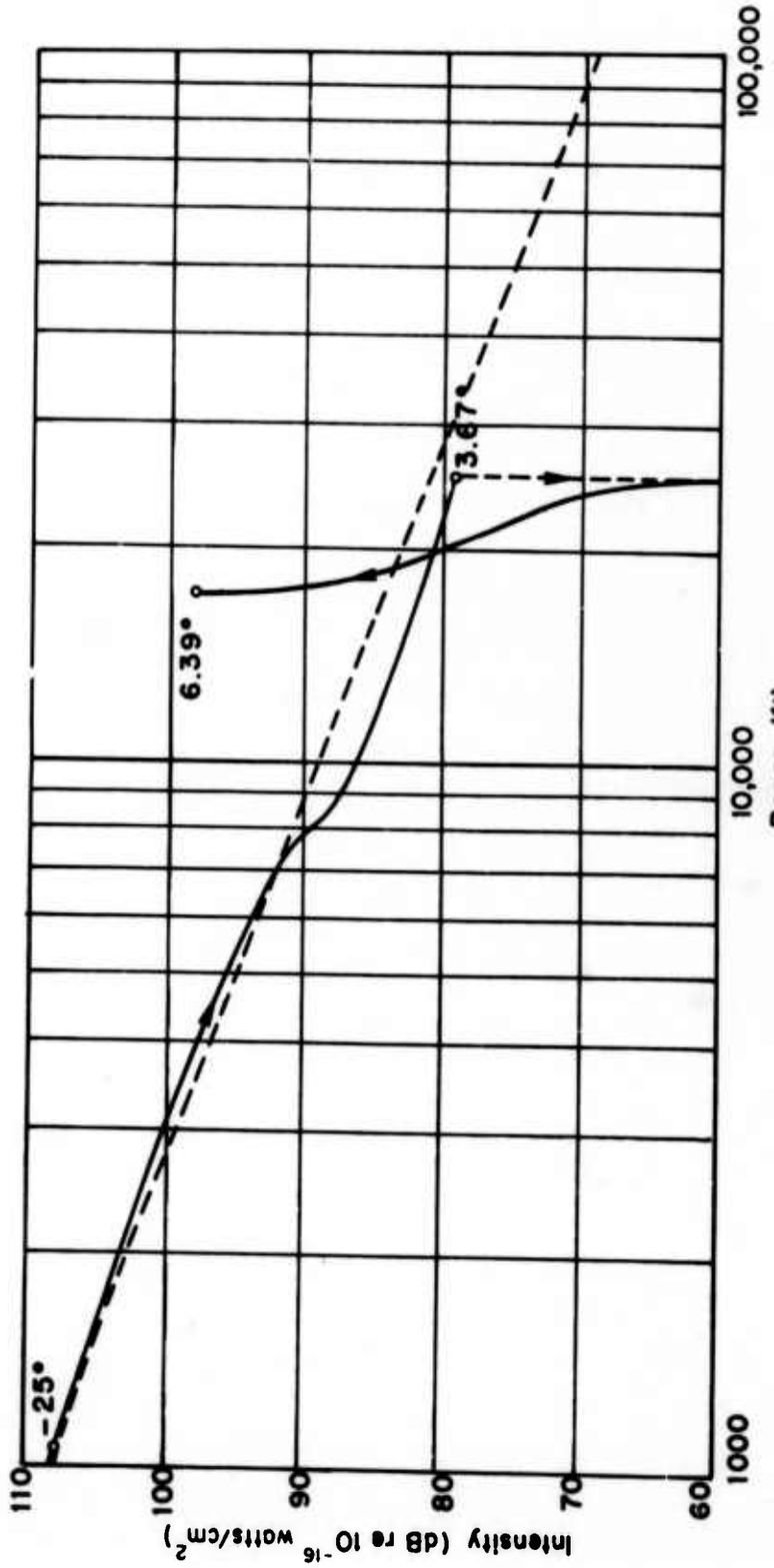

Fig. 27—Intensity variation with range at 90° azimuth (Profile 1)

rays which rise initially to altitudes between 3000 and 4000 ft before returning to ground level at ranges of the order of 70,000 ft. The resulting intensity variation is shown in Fig. 28. Finally, for azimuths beyond about 270 deg the intensity curves again take on the form shown in Fig. 25.

Profile 2

In Fig. 29 the plots of $v + w_x$ at 30-deg increments in azimuth are shown for Profile 2. For azimuths between 0 and 90 deg the intensity variation is similar to that shown in Example 5 and results from the decrease in gradient at the 656-ft level. Figure 30 is typical of this range of azimuth angles.

For azimuth angles from about 120 deg up to 210 deg the resulting intensity curves are again similar to Example 3 in the upwind direction, with a shadow zone at ranges beyond 5000 to 8000 ft.

For azimuths between 240 and 270 deg the higher value of $v + w_x$ at altitudes between 1000 and 2500 ft results in rays being refracted back to the ground from these altitudes at ranges in excess of 20,000 ft.

Finally, for azimuths between 300 and 360 deg the intensity curves are similar to that shown in Fig. 30 but with an additional low intensity branch beyond 16,500 ft range resulting from transmission through the very slight positive gradient between 1148 and 2625 ft, as shown in Fig. 31.

Profile 3

For Profile 3 the altitude dependence of $v + w_x$ at 30-deg increments in azimuth is shown in Fig. 32.

For azimuth angles between 0 and 60 deg the intensity variation is similar to that shown in Example 5 due to the decrease in gradient at the 656-ft level. Figure 33 shows the variation for 60-deg azimuth. The maximum range of 41,289 ft corresponds to a ray with a maximum altitude of 1640 ft, and any ray which exceeds this altitude is in a region of negative gradient and cannot return to the ground level.

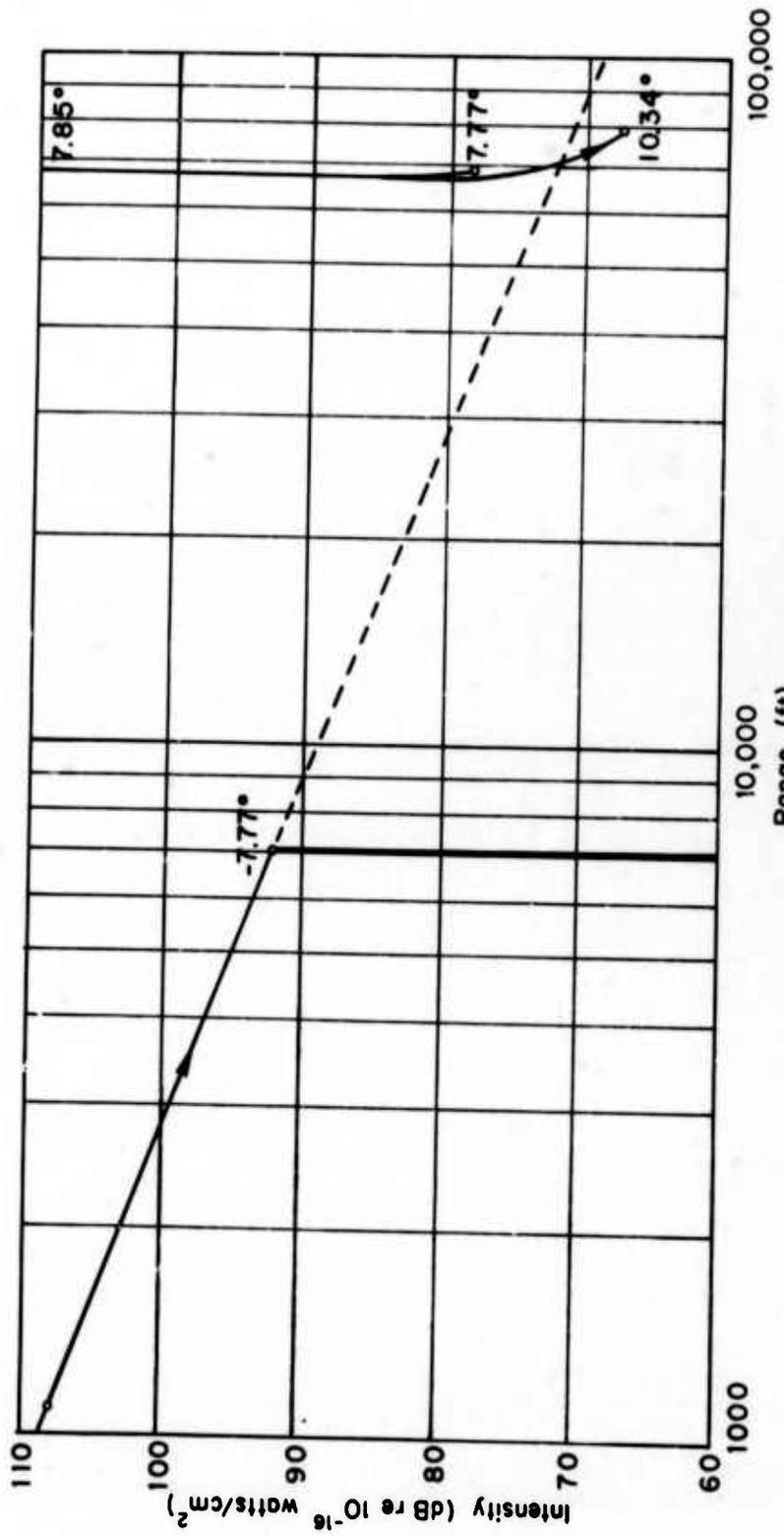

Fig. 28—Intensity variation with range at 240° azimuth (Profile 1)

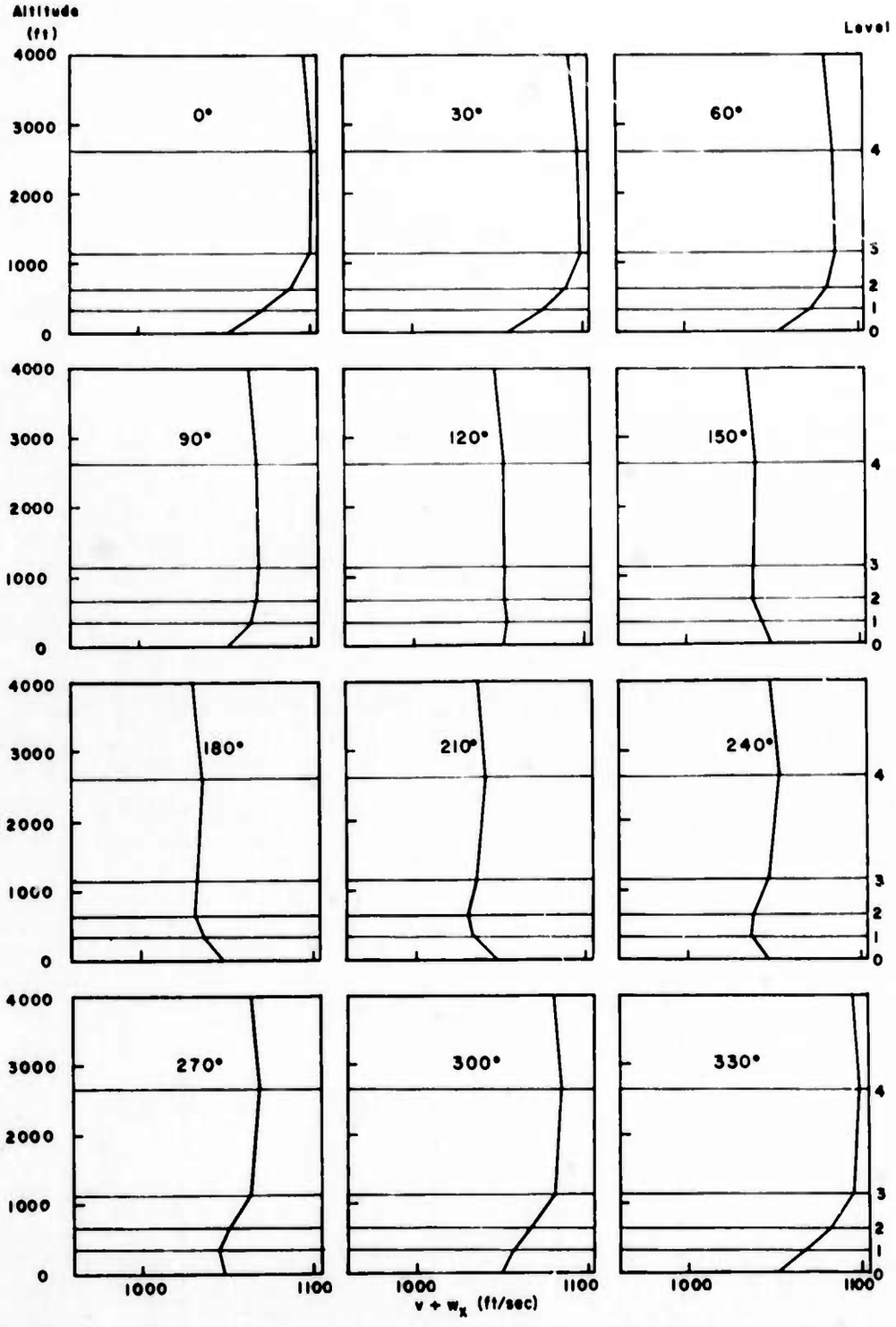

Fig. 29—Dependence of $v + w_x$ on altitude at 30° intervals in azimuth of propagation (Profile 2)

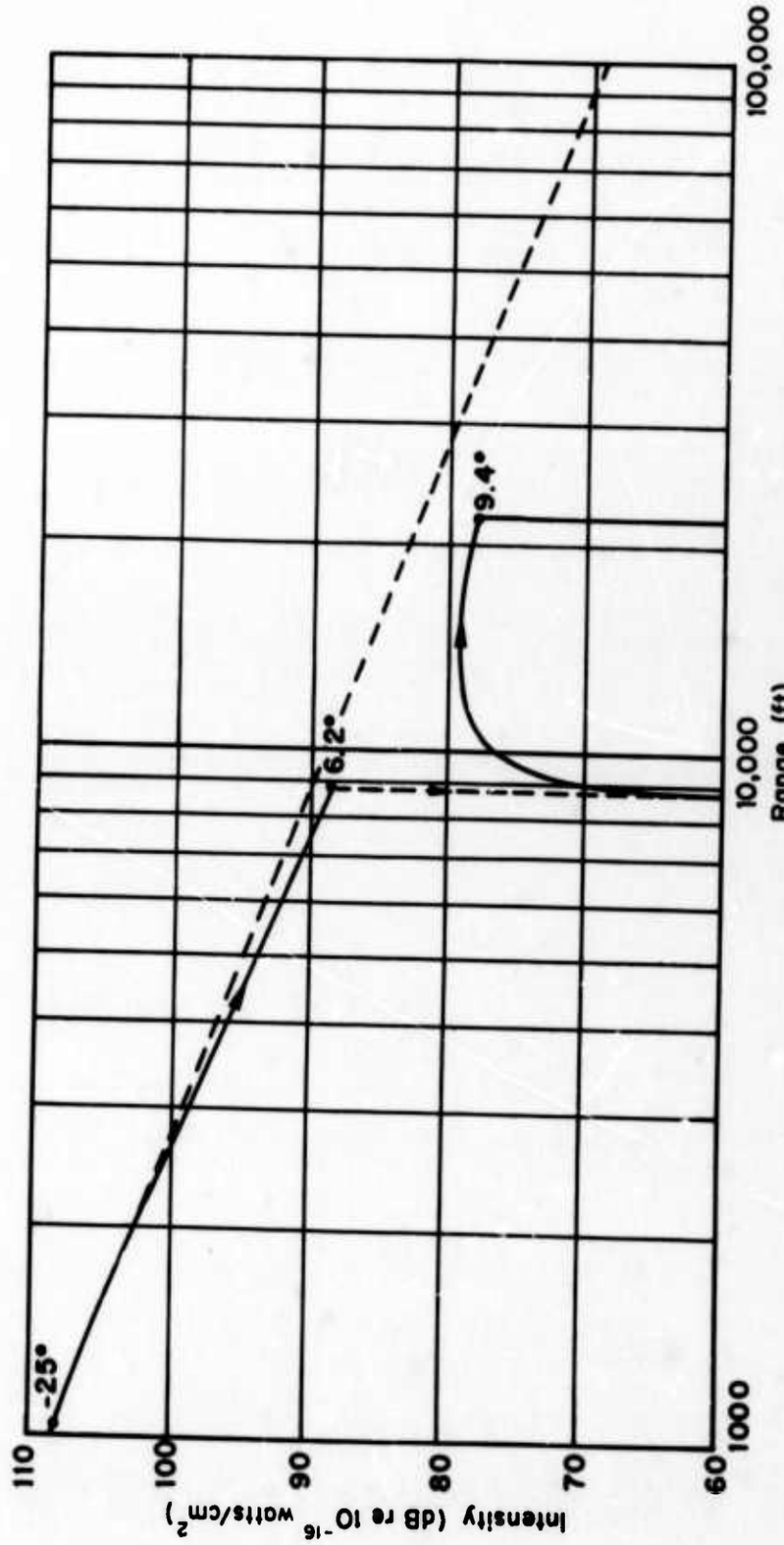

Fig. 30—Intensity variation with range at 30° azimuth (Profile 2)

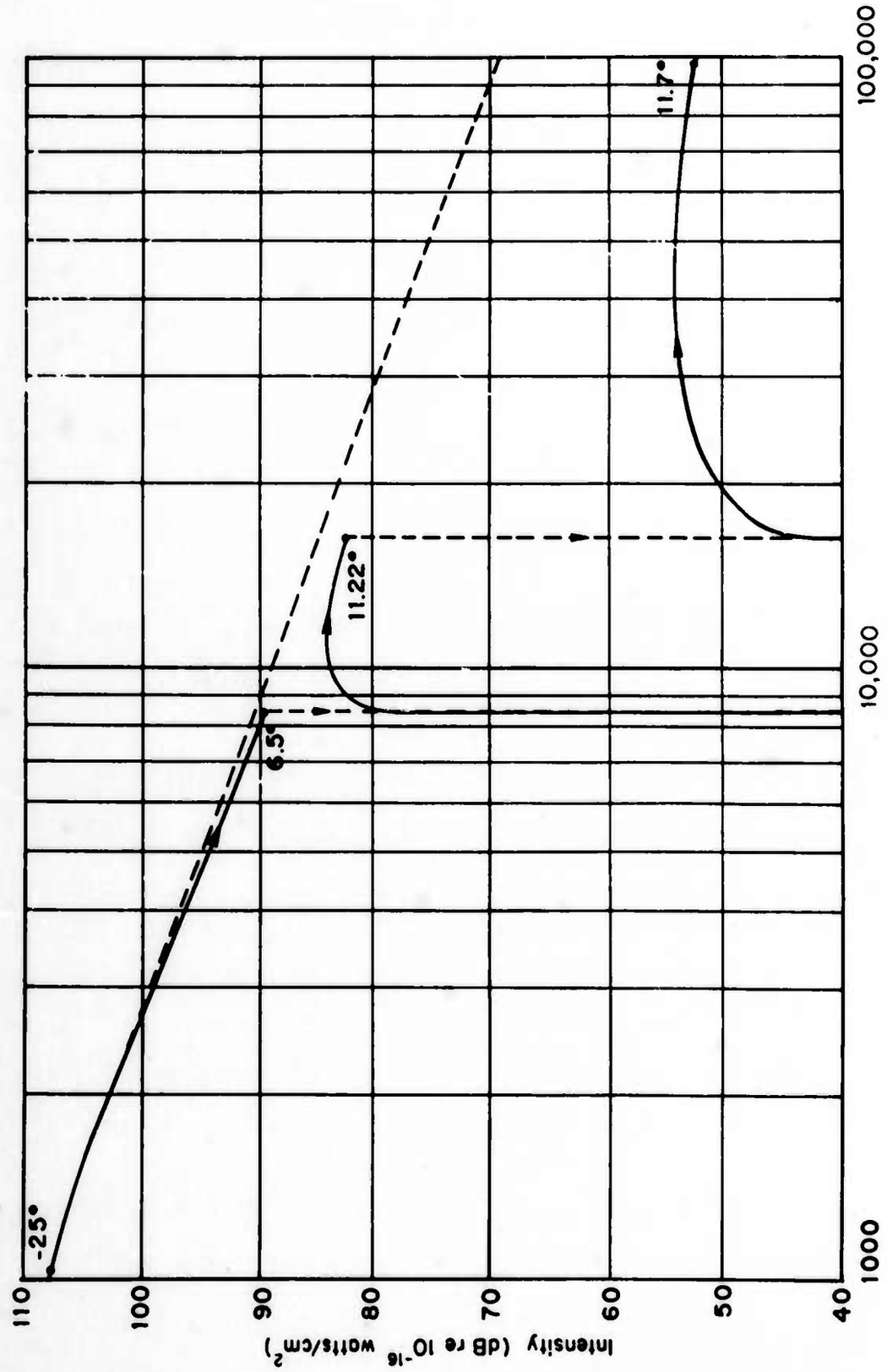

Fig. 31—Intensity variation with range at 330° azimuth (Profile 2)

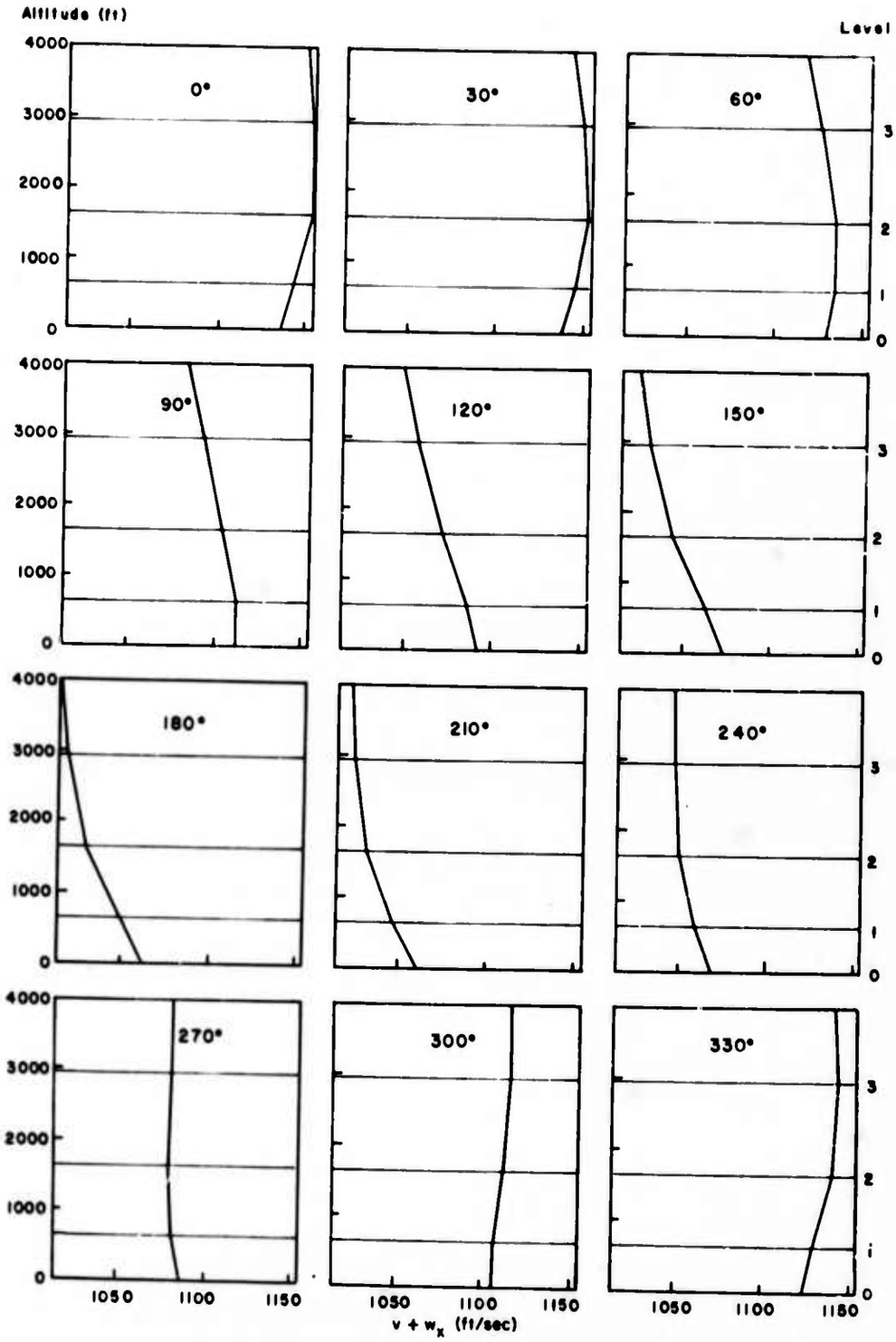

Fig. 32—Dependence of $v + w_x$ on altitude at 30° intervals in azimuth of propagation (Profile 3)

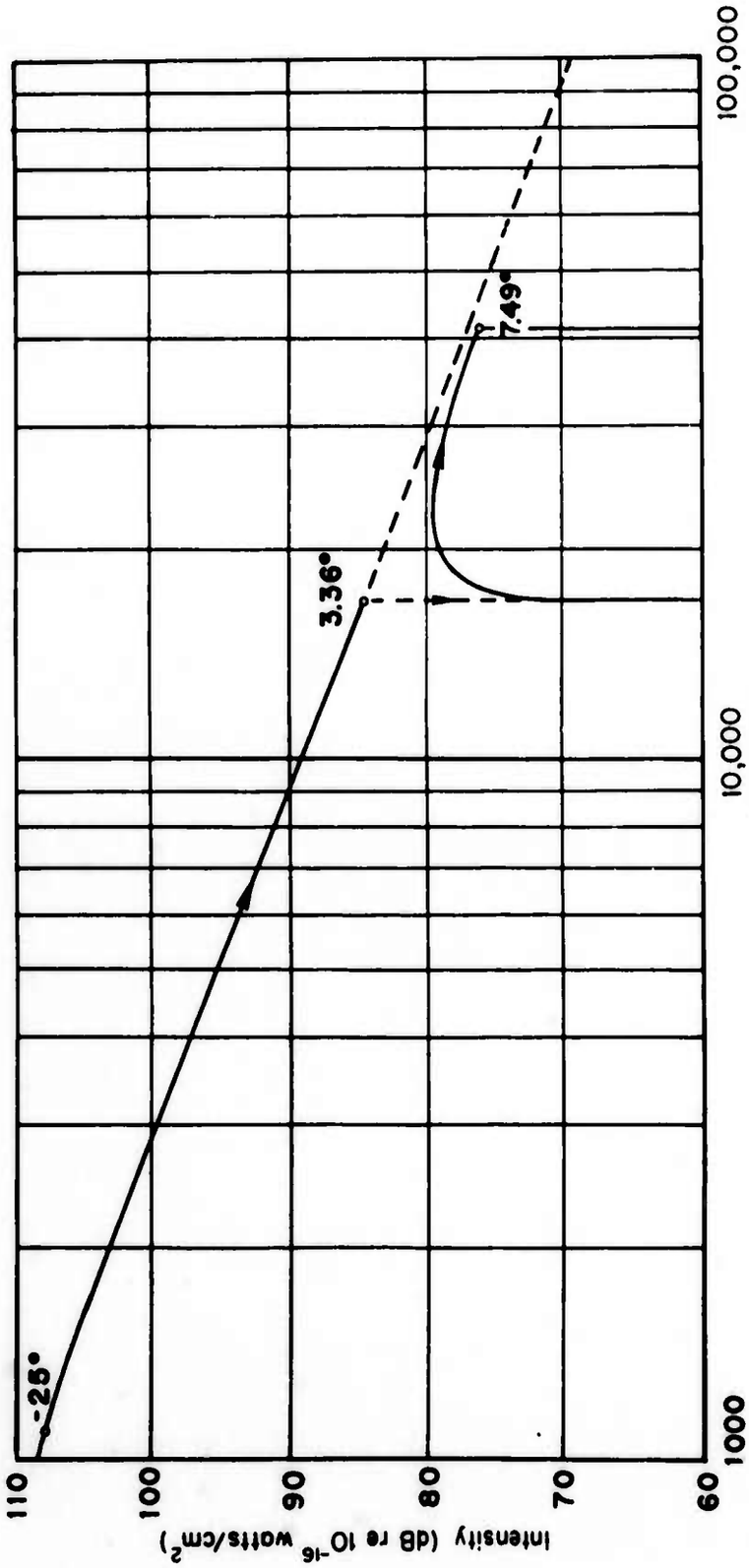

Fig. 33—Intensity variation with range at 30° azimuth (Profile 3)

For azimuths between 90 and 270 deg the gradient is negative at all altitudes and a shadow zone is formed similar to that in Example 3.

Finally, for azimuths between 270 and 360 deg there is a possibility of an enhancement of intensity similar to that in Example 4 due to the increase in gradient at the 656-ft level and a reduction of intensity similar to that in Example 5 due to the decrease in gradient at 1640 ft. This is illustrated in Fig. 34.

ATTENUATION EFFECTS

It is found that the classical attenuation due to viscosity and heat conduction is negligible in comparison with that due to molecular absorption. In Tables 4, 5, and 6 the average temperature and humidity in each atmospheric layer and the molecular absorption coefficients for frequencies of 125, 250, 500, and 1000 cps are presented for each of the meteorological profiles.

An examination of Table 4 shows that for the low water content of the atmosphere at these temperatures, the resulting molecular attenuation is less than 0.1 dB per 1000 ft even at a frequency of 1000 cps. Thus the variation of intensity with distance is essentially independent of frequency for Profile 1.

A similar examination of Table 6 shows that the attenuation increases with both frequency and altitude. However, since the sound rays which reach the ground from the assumed 500-ft source altitude never reach layers 4, 5, or 6, the higher values of attenuation are not encountered. Figure 35 shows the variation of intensity with distance for frequencies of 125 and 1000 cps for the attenuation shown in Table 6. In this case the sound rays are confined to the first two layers of the atmosphere where the attenuation of the 125-cps frequency is about 0.01 dB per 1000 ft while that for 1000 cps is from 0.35 to 0.48 dB per 1000 ft. Thus at the longer ranges the 1000-cps curve lies 10 to 15 dB below that for the lower frequency.

In the case of Profile 2 as shown in Table 5, the combination of temperature and humidity results in comparatively high attenuation at all altitudes, ranging from about 0.15 dB/1000 ft at 125 cps to about 4 dB/1000 ft at 1000 cps. Figure 36 shows an example of the variation

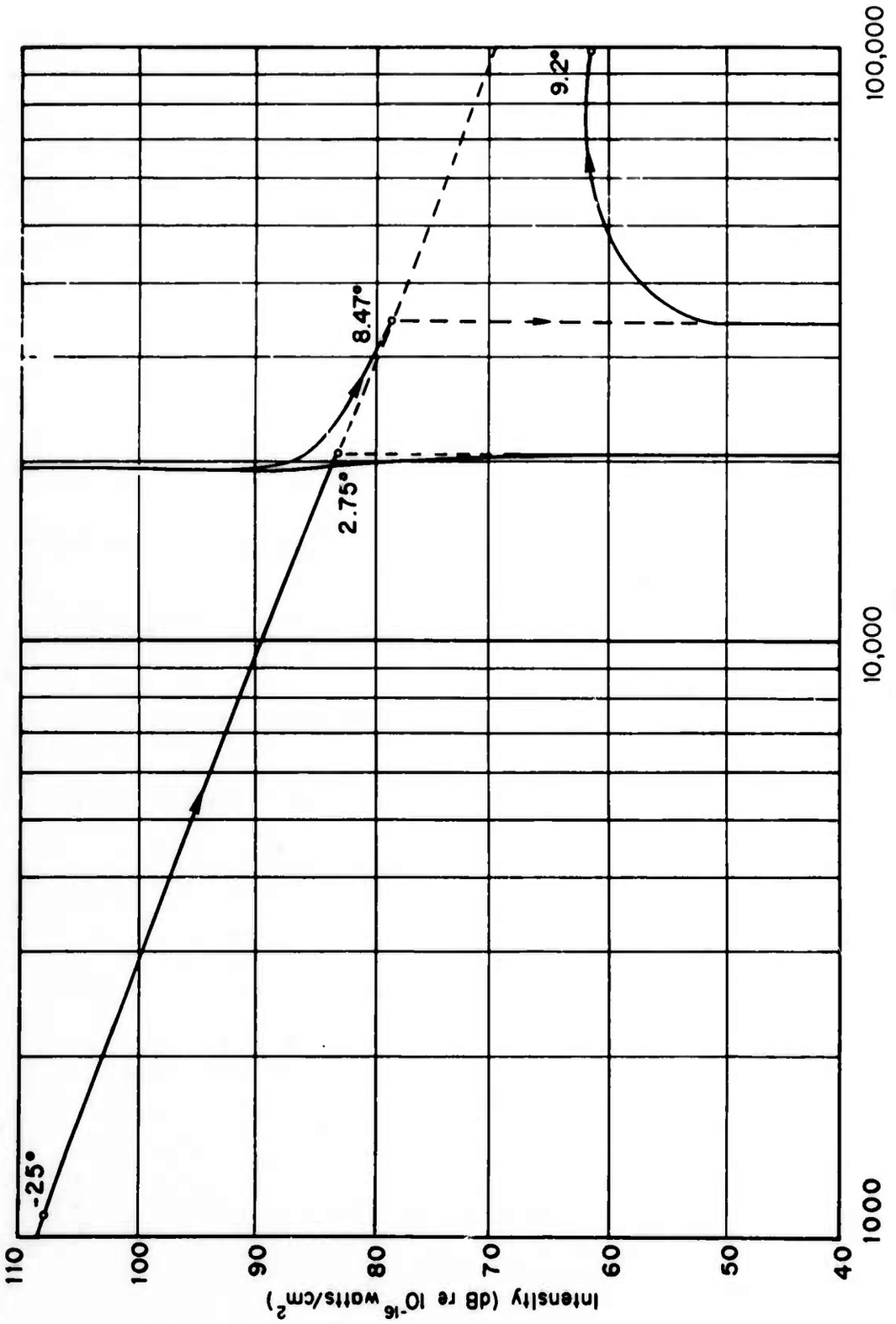

Fig. 34—Intensity variation with range at 330° azimuth (Profile 3)

Table 4

ATMOSPHERIC ATTENUATION FOR PROFILE 1

Layer	Relative Humidity (%)	Temperature (deg C)	Attenuation Coefficient (dB/kft)			
			125 cps	250 cps	500 cps	1000 cps
1	32.5	-36.6	0.0077	0.0077	0.0077	0.0077
2	37.5	-35.6	0.0129	0.0129	0.0129	0.0129
3	41.5	-34.1	0.0221	0.0221	0.0221	0.0221
4	50.0	-32.1	0.0499	0.0502	0.0502	0.0502
5	55.0	-30.1	0.0933	0.0946	0.0949	0.0950
6	47.0	-29.6	0.0767	0.0774	0.0776	0.0776
7	34.5	-31.4	0.0282	0.0283	0.0283	0.0283

Table 5

ATMOSPHERIC ATTENUATION FOR PROFILE 2

Layer	Relative Humidity (%)	Temperature (deg C)	Attenuation Coefficient (dB/kft)			
			125 cps	250 cps	500 cps	1000 cps
1	93.0	-17.0	0.1831	0.6601	1.8927	3.5498
2	93.0	-14.6	0.1250	0.4787	1.6353	4.1298
3	93.0	-11.8	0.0773	0.3045	1.1511	3.7739
4	93.0	-9.6	0.0534	0.2122	0.8278	3.0135
5	91.5	-15.2	0.1409	0.5325	1.7447	4.0492

Table 6

ATMOSPHERIC ATTENUATION FOR PROFILE 3

Layer	Relative Humidity (%)	Temperature (deg C)	Attenuation Coefficient (dB/kft)			
			125 cps	250 cps	500 cps	1000 cps
1	79.3	5.1	0.0056	0.0222	0.0889	0.3552
2	79.8	3.4	0.0075	0.0298	0.1194	0.4769
3	80.5	0.9	0.0113	0.0450	0.1800	0.7180
4	81.8	-1.8	0.0177	0.0706	0.2820	1.1191
5	83.8	-6.7	0.0392	0.1565	0.6185	2.3619
6	85.0	-11.4	0.0862	0.3387	1.2649	3.9991

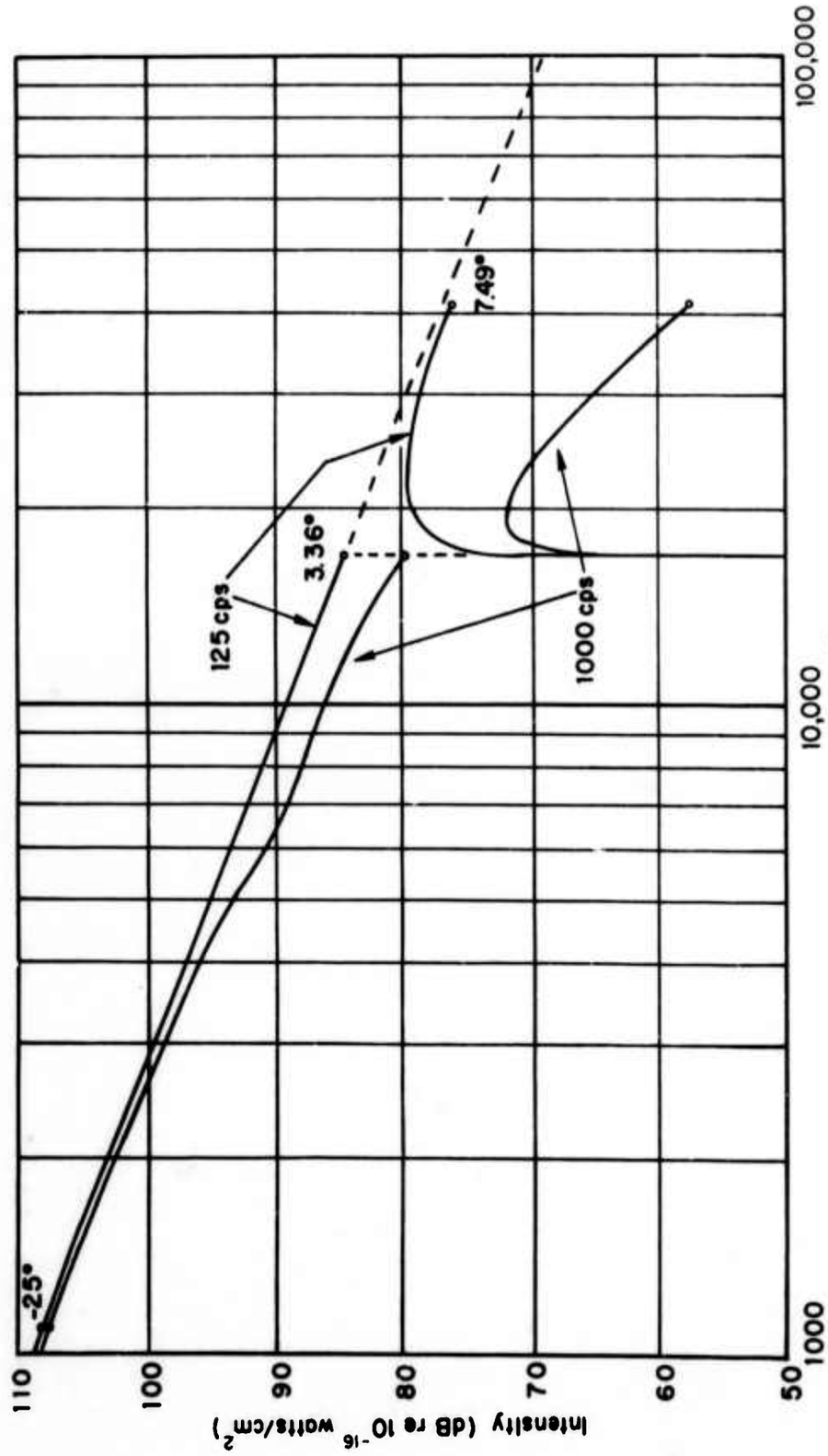

Fig. 35—Intensity variation with range at 30° azimuth for frequencies of 125 and 1000 cps (Profile 3)

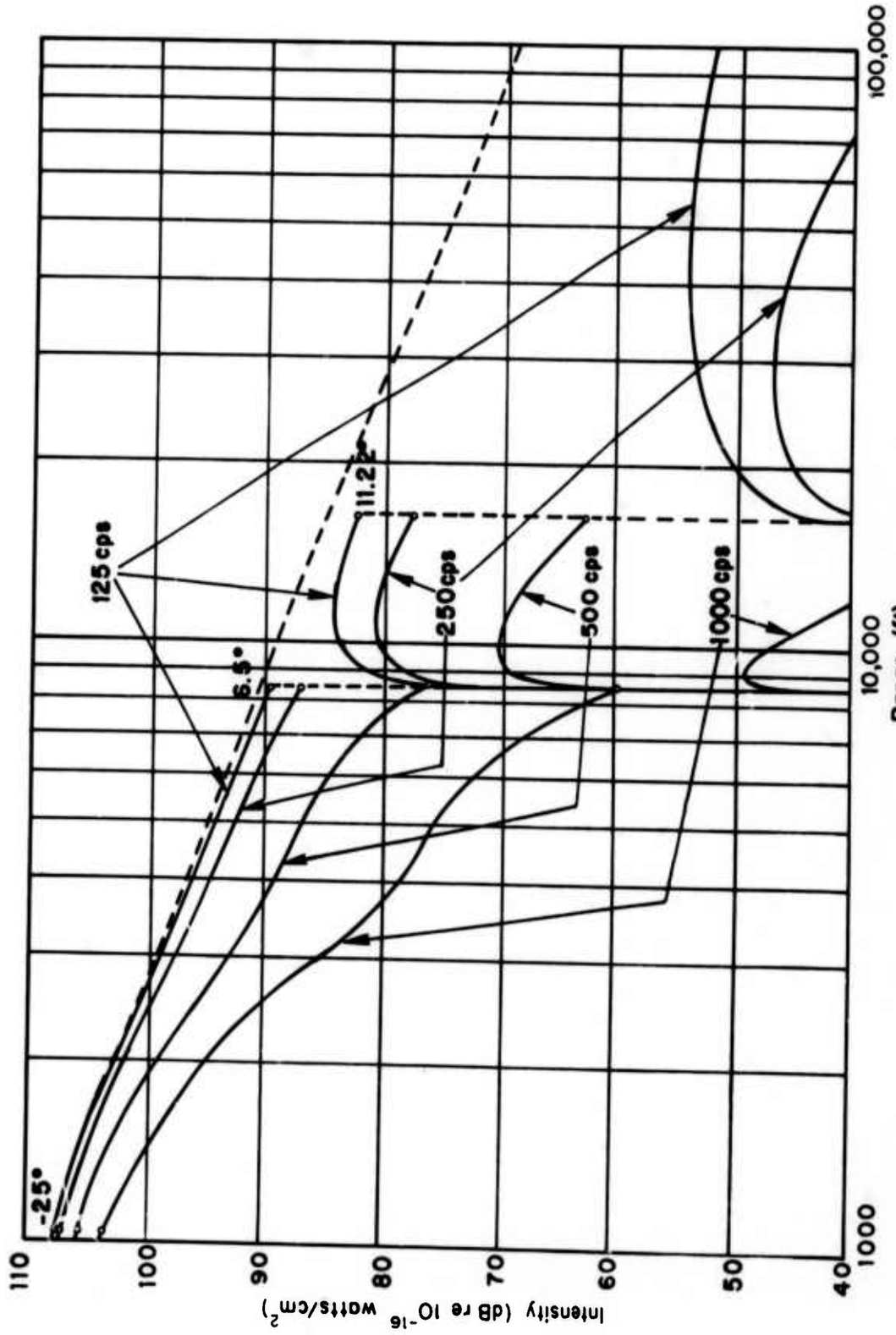

Fig. 36—Intensity variation with range at 330° azimuth for frequencies of 125, 250, 500 and 1000 cps (Profile 2)

of intensity with distance for frequencies of 125, 250, 500 and 1000 cps. It is seen that even at a range of 8500 ft there is a difference of 30 dB between the 125-cps curve and that for 1000 cps.

IV. CONCLUSIONS

On the basis of the foregoing results the following specific conclusions can be stated regarding sound propagation from an elevated source to the ground.

- o A sound ray emanating from an elevated source with an initial inclination angle less than or equal to zero will reach ground level if its refraction constant C (see Eq. (11)) is greater than the maximum value of $v + w_x$ existing between the source and the ground.
- o A sound ray with an initial inclination greater than zero will reach ground level if its value of C not only satisfies the previous condition but also is less than the maximum value of $v + w_x$ occurring above the source.
- o If a ray has an initial elevation angle less than zero and its value of C is equal to the maximum value of $v + w_x$ existing below the source, then its ground range represents the boundary of a shadow zone. Propagation of acoustic energy beyond this boundary can occur only by scattering and diffraction and its intensity drops off quite rapidly with distance beyond the boundary.
- o If the maximum value of $v + w_x$ as a function of altitude occurs above the source then a ray with a positive elevation angle and a value of C equal to this maximum has a ground range which represents the maximum range of direct acoustical propagation.
- o Variations of $v + w_x$ between source altitude and the ground appear to have relatively little effect on the intensity at ground level. Thus in that area of the ground illuminated by rays whose initial elevation angles are negative the intensity variation with distance deviates very little from the inverse-square law.
- o If the gradient of $v + w_x$ decreases discontinuously at some altitude above the source, then the intensity at ground level in the vicinity of those rays which just penetrate the upper layer will be abnormally low.

- If the gradient of $v + w_x$ increases discontinuously at some altitude above the source, the intensity at ground level in the vicinity of those rays which just penetrate the upper layer will be abnormally high.
- Atmospheric attenuation reduces the intensity of the higher frequency components significantly but has comparatively little effect at frequencies of the order of 125 cps, which are readily available in the spectrum of multi-engine jet aircraft.
- For the assumed source altitude of 500 ft and for the three meteorological conditions selected the source could be heard at ground level out to at least 6000 ft in any direction. However, this value would increase with source altitude and with source power and would vary with azimuth of propagation depending on the wind structure. As a result it is extremely difficult to specify a detection range for a ground-based acoustic sensor used to detect elevated targets.

REFERENCES

1. Rayleigh, J.W.S., Theory of Sound, Vol. 2, Dover Publications, Inc., New York, 1945.

2. Fowler, R. H., Statistical Mechanics, Second Edition, Cambridge University Press, London, 1936.

3. Knudsen, V. O., "The Absorption of Sound in Air, in Oxygen, and in Nitrogen--Effects of Humidity and Temperature," J. Acoust. Soc. Am., Vol. V, pp. 112-121, October 1933.

4. Kneser, H. O., "The Interpretation of the Anomalous Sound-Absorption in Air and Oxygen in Terms of Molecular Collisions," J. Acoust. Soc. Am., Vol. V, pp. 122-126, October 1933.

5. Harris, C. M., Handbook of Noise Control, McGraw-Hill Book Co., New York, 1957.

6. Pridmore-Brown, D. C., and Uno Ingard, Tentative Method for Calculating the Sound Field about a Source over Ground Considering Diffraction and Scattering into Shadow Zones, Massachusetts Institute of Technology, NASA Tech. Note 3779, September 1956.

7. Pridmore-Brown, D. C., and Uno Ingard, "Sound Propagation into the Shadow Zone in a Temperature-Stratified Atmosphere above a Plane Boundary," J. Acoust. Soc. Am., Vol. 27, pp. 36-42, January 1955.

8. Batten, E. S., and C. Schutz, Meteorological Conditions Affecting Arctic Sound Transmission, The RAND Corporation, RM-5714-PR, November 1968.

DOCUMENT CONTROL DATA

1. ORIGINATING ACTIVITY	2a. REPORT SECURITY CLASSIFICATION
THE RAND CORPORATION	UNCLASSIFIED
	2b. GROUP

3. REPORT TITLE

PROPAGATION OF SOUND AS AFFECTED BY WIND AND TEMPERATURE GRADIENTS

4. AUTHOR(S) (Last name, first name, initial)

Frick, R. H.

5. REPORT DATE	6a. TOTAL No. OF PAGES	6b. No. OF REFS.
July 1969	95	8
7. CONTRACT OR GRANT No.	8. ORIGINATOR'S REPORT No.	
DAHC15 67 C 0141	RM-5830-ARPA	

9a. AVAILABILITY/LIMITATION NOTICES	9b. SPONSORING AGENCY
---	Advanced Research Projects Agency

10. ABSTRACT

An analysis of the effect of atmospheric conditions on the acoustic detection of low-flying aircraft. For a given position at ground level, the problem is to determine the sound intensity resulting from a sound source of known acoustical power at specified altitude, range, and direction relative to the observer. A stratified atmosphere is assumed in which the temperature, wind velocity, and humidity are dependent on the altitude only. Specification of a refraction law for the sound ray emanating from the elevated source is followed by development of a three-dimensional ray-tracing program to determine the ground-level sound intensity due to a source at an altitude of 500 ft radiating 100 kW (134 HP) of acoustical power. The analysis reveals that the detection range of an elevated source is extremely sensitive to azimuth of propagation as well as to source altitude, power, and frequency.

11. KEY WORDS

Wave propagation
Sound
Atmosphere
Meteorology
Reconnaissance
Intelligence
Detection
Interception
Sensors